Title

Development of brain systems for nonsymbolic numerosity and the relationship to formal math academic achievement

Journal

Human Brain Mapping, 36(2)

ISSN

10659471

Authors

Haist, Frank
Wazny, Jarnet H
Toomarian, Elizabeth
et al.

Publication Date

2015-02-01

DOI

10.1002/hbm.22666

Peer reviewed

HHS Public Access

Author manuscript

Hum Brain Mapp. Author manuscript; available in PMC 2015 June 23.

Published in final edited form as:

Hum Brain Mapp. 2015 February ; 36(2): 804–826. doi:10.1002/hbm.22666.

Development of brain systems for nonsymbolic numerosity and the relationship to formal math academic achievement

Frank Haist[1,2,3,*], **Jarnet H. Wazny**[2], **Elizabeth Toomarian**[2], and **Maha Adamo**[2]

[1]Department of Psychiatry, University of California, San Diego, 9500 Gilman Drive, La Jolla, CA 92093-0115 USA

[2]Center for Human Development, University of California, San Diego, 9500 Gilman Drive, La Jolla, CA 92093-0115 USA

[3]Kavli Institute of Brain and Mind, University of California, San Diego, 9500 Gilman Drive, La Jolla, CA 92093 USA

Abstract

A central question in cognitive and educational neuroscience is whether brain operations supporting non-linguistic intuitive number sense (numerosity) predict individual acquisition and academic achievement for symbolic or "formal" math knowledge. Here, we conducted a developmental functional MRI study of nonsymbolic numerosity task performance in 44 participants including 14 school age children (6–12 years-old), 14 adolescents (13–17 years-old), and 16 adults and compared a brain activity measure of numerosity precision to scores from the Woodcock-Johnson III Broad Math index of math academic achievement. Accuracy and reaction time from the numerosity task did not reliably predict formal math achievement. We found a significant positive developmental trend for improved numerosity precision in the parietal cortex and intraparietal sulcus (IPS) specifically. Controlling for age and overall cognitive ability, we found a reliable positive relationship between individual math achievement scores and parietal lobe activity only in children. In addition, children showed robust positive relationships between math achievement and numerosity precision within ventral stream processing areas bilaterally. The pattern of results suggests a dynamic developmental trajectory for visual discrimination strategies that predict the acquisition of formal math knowledge. In adults, the efficiency of visual discrimination marked by numerosity acuity in ventral occipital-temporal cortex and hippocampus differentiated individuals with better or worse formal math achievement, respectively. Overall, these results suggest that two different brain systems for nonsymbolic numerosity acuity may contribute to individual differences in math achievement and that the contribution of these systems differs across development.

Keywords

child development; adolescent development; academic achievement; mathematics; functional magnetic resonance imaging; cognition; behavior; number sense; numerosity

Senior Author Information: Frank Haist, Ph.D., Department of Psychiatry & Center for Human Development, University of California, San Diego, 9500 Gilman Drive, MC 0115, La Jolla, CA 92093-0115 USA, fhaist@ucsd.edu, Phone: +1 858-822-5456.

The authors declare no conflict of interest.

1. Introduction

An intuitive sense of quantities and their relationships is a primitive ability humans share with many other species (for reviews, see Agrillo, 2012; Brannon, 2006; Dehaene, 1992; Dehaene, 2011). For example, we can estimate the relative wealth of players at a casino simply by comparing chip stacks, or quickly assess the shortest security check-in line at the airport. This cognitive ability, often referred to as numerosity, depends on an *approximate number system* (ANS) that operates independently of linguistic or symbolic representations of numbers (e.g., Gordon, 2004; McCrink and Wynn, 2007; Spaepen, et al., 2011; Xu and Spelke, 2000). In humans and non-human primates, ANS operations depend critically on activity localized to the lateral parietal cortex (Cantlon, et al., 2009b; Nieder and Dehaene, 2009; Roitman, et al., 2012); specifically in humans, this activity has been observed in the intraparietal sulcus (IPS) region bounded by the inferior (IPL) and superior (SPL) parietal lobules (Dehaene, 2011; Dehaene, et al., 2003; Nieder, 2013).

It is important to consider two basic properties of the ANS. First, the operations of the ANS are observed most reliably when estimating magnitudes greater than three or four items; estimating fewer items falls within the subitizing range (Kaufman and Lord, 1949) and may default to an automatic counting strategy (Choo and Franconeri, 2014; for review, see Hyde, 2011; Simon and Vaishnavi, 1996). Second, the ANS is sensitive to numerical distance and magnitude. Distance refers to the absolute difference between contrasted quantities. For example, accuracy is greater and reaction time shorter when judging the greater quantity between 12 blue and 3 yellow dots displayed on a computer screen than when judging between 6 blue and 3 yellow dots. Given the same distance, accuracy is greater and reaction time shorter when discriminating sets of lower magnitude, such as 6 blue and 3 yellow dots (ratio = 2.0), than when the magnitudes are greater, such as 18 blue and 15 yellow dots (ratio = 1.2). Distance and magnitude interact within the ANS following Weber's Law, such that accuracy and reaction time vary as a function of the ratio between the numerical sets (see Roitman, et al., 2012). Differences in ANS precision drive accuracy and reaction time variations between individuals. Researchers often use behavioral ratio effects (BRE) or FMRI BOLD signal neural ratio effects (NRE) as measures of ANS precision to evaluate correlations to math achievement (Bugden, et al., 2012; Cantlon, et al., 2009a; Cohen Kadosh, et al., 2007; Holloway and Ansari, 2010; Libertus, et al., 2007; Piazza, et al., 2007; Pinel, et al., 2001; Price, et al., 2013).

The nonsymbolic BRE, as frequently measured by dot magnitude comparison tasks, shows monotonic improvement from childhood through the third decade of life (Halberda, et al., 2012). A number of studies have shown correlations between behavioral ANS acuity and math achievement, particularly in early childhood (Castronovo and Gobel, 2012; Halberda and Feigenson, 2008; Halberda, et al., 2008; Libertus, et al., 2011; Libertus, et al., 2012; Mazzocco, et al., 2011; Xu and Spelke, 2000). Nonetheless, for each study of children and/or adults showing a correlation between nonsymbolic ANS acuity and math achievement or knowledge, an equal number fail to find such a link (De Smedt, et al., 2013). In contrast, the an overwhelming number of studies using symbolic comparison tasks, such as those presenting Arabic numerals rather than dot arrays, produce positive correlations

with math achievement and knowledge tests (for review, see De Smedt, et al., 2013). There is an increasingly prevalent view that nonsymbolic ANS operations generally support "informal" math abilities including counting, magnitude comparisons, and non-verbal addition and subtraction, but do not significantly contribute to "formal" math operations such as abstract number symbol manipulations and math rule applications (Inglis, et al., 2011; Libertus, et al., 2013; Price, et al., 2012; Sasanguie, et al., 2013). Operations engaged by symbolic tasks are proposed to be better predictors of formal math skills (De Smedt, et al., 2013).

This raises at least two possible explanations for a correlation between nonsymbolic ANS functions and formal math achievement. One possibility is that such findings are linked to specific methodological approaches for estimating nonsymbolic ANS precision coupled with particular estimates of formal math achievement. Thus, the findings may be limited to a specific task-achievement association. De Smedt and colleagues (2013) considered and dismissed this possibility because no systematic differences in methods or approaches between nonsymbolic ANS studies could be ascertained from studies finding significant correlations to math achievement and those that did not. Alternatively, perhaps associations between formal math achievement and performance on nonsymbolic magnitude estimation tasks arise because there is more than one brain system engaged during numerosity tasks and the operations of a second system may influence the correlation.

Functional neuroimaging across development optimally test this possibility because the operations of the nonsymbolic ANS are so tightly linked to operations within the lateral parietal lobe in general and the IPS specifically (for reviews, see Ansari, 2008; Butterworth and Walsh, 2011; Cantlon, 2012; for other views, see Cohen Kadosh, et al., 2008a; de Hevia, et al., 2008; Dehaene, 2011; Dehaene, et al., 2003; Dormal, et al., 2012a; Henik, et al., 2011; Nieder, 2013; Walsh, 2003). There is a clear developmental trajectory for IPS activity during nonsymbolic magnitude estimation. Several studies report greater IPS involvement in adults as compared to children ranging in age from 4 to 12 years (Ansari and Dhital, 2006; Cantlon, et al., 2006; Cantlon, et al., 2009a; Holloway and Ansari, 2010; Kaufmann, et al., 2008; Kovas, et al., 2009; Kucian, et al., 2008). Developmental FMRI evidence linking IPS activity to individual academic math achievement is meager; nonetheless, similar to the behavioral literature, the available data suggest that the strongest associations are found with symbolic tasks (Bugden, et al., 2012; Price, et al., 2013). Based on the present state of the field, De Smedt et al. (2013; Fazio, et al., 2014; see also, Kaufmann, et al., 2011) concluded "To the best of our knowledge there does not exist a study that reveals an association between brain activation during nonsymbolic number processing and individual differences in mathematical achievement in typically developing children" (p. 51).

Here, we report results from a study evaluating this precise issue. Using FMRI, we tested a nonsymbolic dot magnitude comparison task using stimuli derived from the Panamath task (http://panamath.org) in which the dot ratios varied parametrically with 44 typically developing participants ages 6 to 34 years. In addition, we collected standardized math and reading achievement data, and measures of overall cognitive ability as assessed by a standardized IQ test. A voxelwise BOLD signal neural ratio effect (NRE) was calculated for

each participant to identify brain areas responding to the parametric differences in numerosity ratios. Critically, we approached our analyses using whole-brain regression statistics to evaluate developmental effects across the entire age range, as well as within divisions of child, adolescent, and adult age groups.

2. Material and Methods

2.1 Participants

Twenty-one children (6 to 12 years), 16 adolescents (13 to 17 years), and 16 adults (18 to 34 years) initially participated in this experiment. Three children were excluded for excessive motion during the task, one child for the inability to complete the task, one adolescent for a technical problem during scanning, and three children and one adolescent for performance that fell more than 2.5 SDs below the mean group performance on one or more of the numerosity ratio ranges used. See fMRI Data Processing and Analysis section for description of exclusion criteria based on movement and artifact. The final participant sample was comprised of 14 children, 14 adolescents, and 16 adults (see Table for demographic information). One child did not complete the academic achievement testing and was not included in those regression analyses. Thirty-nine of the 44 participants were right-handed as determined by the Edinburgh Handedness Inventory (Oldfield, 1971). All participants had normal or corrected-to-normal vision and no history of psychiatric or neurological disease, significant head trauma, or other known condition that may negatively affect brain function. In addition, overall cognitive abilities of all participants were estimated at average or better as measured by scores on a standardized IQ test (Full Scale IQ score ≥ 90). We recruited research participants from the general San Diego region through advertisements or university affiliation. The Human Research Protections Program of the University of California, San Diego approved this study. Participants or their parent/guardian provided informed consent before the study and were paid or given course credit for participation. Children and adolescents provided assent before participation.

2.2 Stimuli

We created 384 bitmap numerosity stimulus images, plus additional stimuli used for training, using Panamath software (http://www.panamath.org) based on ratio settings optimized for 10-year-olds. Task stimuli consisted of a uniformly gray stimulus field (RGB = 128) with randomly arranged yellow dots (RGB = 255/255/0) on the left side and blue dots (RGB = 0/0/255) on the right side. The average dot diameter was 60 pixels with a diameter variation of up to 25% (45 to 75 pixels). The yellow and blue dots overlapped up to 20% at the center of the stimulus field. See Figure 1A for examples of task stimuli. The ratio of the yellow to blue dots formed the task's key independent variable. Four ratio ranges or bins were used: *Lowest ratio bin* = 1.20 to 1.37, *Low ratio bin*: 1.37 to 1.57, *High ratio bin* = 1.63 to 1.87, and *Highest ratio bin* = 2.57 to 2.94. Mask images were comprised of an equal number of randomly arranged blue and yellow 4×4 pixels created using the Scramble plugin for Photoshop (http://www.telegraphics.com.au).

2.3 Design and Procedure

2.3.1 Cognitive and Academic Achievement Testing—All participants were administered the two subtest version of the Wechsler Abbreviated Scale of Intelligence (WASI; Wechsler, 1999) to obtain an estimated Full-Scale IQ (FSIQ). A minimum FSIQ score of 90 was required for participation in the study. Participants were also administered four math achievement subtests (Calculation, Math Fluency, Applied Problems, and Quantitative Concepts) and a reading/phonological achievement subtest (Letter-Word Identification) from the Woodcock-Johnson III Tests of Achievement Normative Update (WJ-III Normative Update; Woodcock, et al., 2007).

2.3.2 Nonsymbolic Magnitude Estimation Task—The nonsymbolic magnitude estimation task was presented in two task runs that used a randomized event-related FMRI design. Each run was comprised of 96 2500 ms stimulus trials, interleaved with 32 2500 ms fixation-only null trials. Additional 7.5 sec and 10 sec fixation-only stimuli were presented at the start and end of the run, respectively. The 96 stimulus trials were comprised of 24 stimuli from each of the four ratio bins. Thus, 192 stimuli were presented over both runs including 48 stimuli from each of the four ratio bins. All stimuli were unique. Each 2500 ms stimulus trial began with the presentation of a fixation cross centered on a gray background (*fixation*) for 300 ms, followed by a 1200 ms stimulus presentation, then a mask image for 200 ms, and ended with a blank gray screen for 800 ms. Null trials consisted of 300 ms of fixation followed by 2200 ms of blank gray screen. Figure 1B presents a graphical depiction of the stimulus and fixation-only null trials. The order of presentation of stimulus and null trials was pseudorandomized. Participants were instructed to press one of two buttons on a fiber optic device with their right hand to indicate which side of the screen contained the greater number of dots, the left side (yellow dots) or right (blue dots). Each task run lasted 5 min 20 sec during which 160 FMRI volumes were obtained (TR = 2000 ms).

All participants received training and practice in the task immediately before the FMRI session. The training task used unique stimuli and presented the ratio stimuli from highest to lowest ratios (i.e., easier to more difficult; Odic, et al., 2014). Computerized auditory feedback was provided during the initial training. Following that training, participants underwent a second phase of training that exactly matched the in-scanner task parameters. Children 12 years and younger were given practice in a simulated MR scanner (i.e., “mock scanner”) that provided familiarization with the scanning environment as well as training in motion compliance prior to their FMRI test session.

2.4 Task Presentation and Image Acquisition

All stimuli were back-projected onto a screen located at the foot of the scanner bed from an LCD projector located in the scanner console room. A computer using Presentation software controlled stimulus presentation and response collection (version 16; http://www.neurobs.com). Participants viewed the stimuli via a mirror attached to the scanner coil above their eyes. Imaging data were obtained at the University of California, San Diego Center for Functional Magnetic Resonance Imaging using a short-bore 3.0 Tesla General Electric Signa EXCITE MR scanner equipped with a parallel-imaging capable GE 8-channel head coil. FMRI data were acquired using a single-shot gradient-recalled echo-planar

imaging sequence with blood oxygenation level-dependent (BOLD) contrast (38 slices; 4-mm slab; gap=0.5 mm, TR=2000; TE=30 ms; flip angle=90°; FOV=256 mm; matrix=64×64; in-plane resolution=4 mm^2). A high-resolution parallel imaging SPGR scan was acquired for anatomical localization (sagittal acquisition; TR=8.11 ms; TE=3.17 msec; TI=600 msec; NEX=1; flip angle=8°; FOV=256 mm; acquisition matrix=256×192; 168 slices; slice thickness=1 mm; resolution=0.98×0.98×1 mm).

2.5 FMRI Data Processing and Analysis

2.5.1 Preprocessing—Processing of the BOLD data incorporated a de-noising technique based on Independent Component Analysis (ICA) to remove structured physiological noise (Perlbarg, et al., 2007), eye motion artifact, and task-negative activation. We have shown previously that this procedure significantly increases the statistical power in developmental studies (Haist, et al., 2013). The first three volumes in each run were deleted to eliminate T1 saturation effects. Each of the FMRI task sequences were motion corrected, slice timing corrected, and spatially smoothed (8 mm FWHM Gaussian filter kernel) using AFNI software (Cox and Hyde, 1997). These data were submitted to single-session independent component analysis (ICA) using FSL MELODIC (Beckmann and Smith, 2004), with the number of output components automatically estimated. De-noising proceeded as follows. ROIs were defined from each individual's anatomy that included the lateral ventricles (ventricle ROI), bilateral areas within both frontal and posterior white matter (white matter ROI), a region anterior to the superior aspects of the pons in the location of the basilar artery (Perlbarg, et al., 2007), and the eyes (Beauchamp, 2003; Haist, et al., 2005; Tregellas, et al., 2002). The BOLD time series were extracted from the raw data for each of these ROIs and served as the dependent variables in separate stepwise multiple regression analyses (forward selection $p < .01$, backward removal $p < .05$) with the set of IC time series serving as the independent variables. The stepwise regression results defined the subset of ICs that significantly predicted signal linked to physiological or eye-motion/blink artifact. This subset of ICs formed the preliminary noise IC dataset. In another analysis, we calculated the Pearson correlation coefficient between each IC and a model of task-related (i.e., task-positive) activation generated by convolving the stimulus time series with a gamma function (Cohen, 1997). Any IC, including ICs not previously identified as part of the noise subset, that was negatively correlated with task at $r \leq -.20$ ($p \leq .01$) was added to the noise subset. This procedure removed task-negative activation in the final BOLD data for a clearer exploration of task-positive activation. The final noise dataset of ICs was filtered from the subsequent reconstruction of each run. Resulting de-noised task runs were signal normalized (mean = 100), registered into standardized MNI space ("Colin 27"; Holmes, et al., 1998), and resampled to 3 mm isotropic voxels.

2.5.2 Inclusion criteria for individual participants and FMRI data scrubbing—The motion correction procedure generated measurements for the required rotation around the *x*, *y*, and *z* axes (i.e., *pitch*, *roll*, and *yaw*; measured in degrees) and translation in *x*, *y*, and *z* (measured in mm) for each volume to register to the standard image (middle volume in the time series). Individual volumes were filtered from the analysis if rotation exceeded 1° or displacement exceeded 1 mm. This is a form of scrubbing procedure (Siegel, et al., 2014). As an additional quality measure, we applied AFNI 3dToutcount to the motion corrected,

slice time resampled, and spatially smoothed data to identify volumes that contained a large number of "outlier" voxels. A large number of outlier voxels may arise from a number of factors including residual uncorrected motion effects or scanner artifact. The program calculated the median absolute deviation (MAD) of the time series minus the linear trend. Outlier voxels were defined as those exceeding the range defined by the formula: $\alpha * \sqrt{\frac{\pi}{2}} * MAD$, where α is the inverse of the reversed Gaussian continuous distribution function scaled by 0.001/N with N being the length of the time series (i.e., 157 volumes). A volume was filtered from the analysis if it contained 10% or more outlier voxels. Our inclusion criteria for individual participants required that the number of filtered volumes be less than 20% of the total number of volumes (i.e., <32 volumes) in both of the task runs; that is, exceeding this threshold in either run eliminated a participant from the study. The strict criteria assured that each participant contributed at least 80% of the available data from each of the two task runs.

2.5.3 Analyses of individual participant FMRI data—The FMRI data from individual participants were analyzed using a deconvolution multiple regression procedure (AFNI 3dDeconvolve). The hemodynamic response function (HRF) for each stimulus in the task was estimated from a series of eight tent basis functions that modeled the post-trial onset window from 0 to 14 seconds. The multiple regression model included the stimulus parameters for correct responses in each of the four ratio bins (Lowest, Low, High, Highest) together with eight nuisance parameters that accounted for all incorrect responses, non-response trials, and six motion artifacts (3 rotation and 3 displacement variables), plus three polynomial factors of no interest (linear, quadratic, and cubic trends). The resulting HRF models for each stimulus category were adjusted to set the HRF initiation to zero. Pilot testing indicated that the peak HRF occurred between 4 and 8 sec; thus, the mean BOLD signal for the 4–8 sec window was calculated for each of the ratio bin categories.

2.5.4 Calculation of Neural Ratio Effect (NRE)—To compute a *neural ratio effect* (NRE) we conducted a voxelwise analysis for an orthogonal linear trend between the four ratio bins using the mean 4–8 sec data. The orthogonal coding yielded positive values for a linear trend that was more active for the lower ratio bins, and negative values for the linear trend that was more active for the higher ratio bins. The resulting voxelwise beta coefficients were used in the FMRI group analyses.

2.5.5 Analysis of Group FMRI Data—All FMRI analyses used the NRE as the dependent measure of BOLD activation to the numerosity task. Developmental trends were analyzed using the natural logarithm of age as a continuous variable in a linear regression analysis. Math achievement was defined by the age-corrected WJ-III Broad Math Index Scaled Score (mean = 100, SD = 15), a measure derived from the four math achievement subtests. Age and math achievement effects were analyzed together in a single repeated-measures ANCOVA using age and math achievement as continuous between-subjects factors. FSIQ and the WJ-III Letter-Word Identification Scaled Score were used as covariates to control for general cognitive abilities and non-math academic achievement, respectively (Thomas, et al., 2009). All FMRI analyses were corrected for Type I errors using a cluster-threshold correction based on a Monte Carlo simulation with a voxelwise

threshold of $p \leq .050$ (two-sided) and a minimum cluster volume of 1350 μl (i.e., 50 contiguous voxels) that resulted in an effective two-sided $\alpha = .050$ (Forman, et al., 1995).

2.4.6 Analysis of motion and scrubbing data—For each participant, the mean correction necessary to register each volume in the time series to the middle volume was calculated for each of the three rotation axes (in degrees) and three translation axes (in mm). The data from all participants were submitted to separate Pearson correlation analyses against age (natural logarithm). Bonferroni correction was used to achieve an overall &*agr;* = .05. Age effects (natural logarithm) in the number of filtered volumes were analyzed using a separate Pearson correlation.

2.6 Analysis of Task Behavioral Data

Accuracy and reaction time to make correct responses within each ratio bin were calculated for each individual. To compute a *behavioral ratio effect* (BRE), orthogonal linear trends were calculated across the four ratio bins for reaction time and accuracy. Thus, the BRE was calculated in a similar manner to the NRE. The orthogonal coding of the BRE produced positive values for a linear trend when reaction times were longest or accuracy lowest for the lower ratio bins relative to the higher ratio bins. The linear trend correlations for each participant were transformed to Fisher *z* scores for group analyses (Fisher, 1924). The relationship between age and math achievement scores with respect to BRE scores were analyzed using Pearson correlation coefficients and repeated-measures ANOVA with BRE as the within-subjects factor and age or math achievement scores as a continuous between subjects factor.

3. Results

3.1 Behavioral results

3.1.1 Age Effects for Reaction Time (RT) and Accuracy—Mean RT and accuracy results from each of the four ratio bins and the mean BRE score from the numerosity task are shown in Figure 2. Because of outstanding questions in the literature about some numerosity and achievement effects being limited to children, results are also described for the three age groups separately (i.e., adults, adolescents, and children). The natural logarithm of age was used in all analyses to better meet the assumption of linearity within general linear model analyses (Neter, et al., 1996).

As can be seen in the left panel of Fig. 2, mean RT across the ratio bins for the full sample and all three age groups showed a monotonic change in RT as a function of ratio, with the longer RTs for the more difficult lower ratio comparisons compared to easier higher ratio comparisons. The mean RT BRE scores were all significantly above zero, indicating that the linear trend for RT was significant in all contrasts, ts ≥ 8.235, ps ≤ .001 (one-tailed), and the variance accounted by the mean linear trends was high: full sample $R^2 = .934$; adult $R^2 = .968$, adolescent $R^2 = .935$; child $R^2 = .878$. In summary, the full sample and all three groups showed a reliable BRE indicating that RT was a sensitive measure of the ratio manipulation.

Age effects from the full sample were analyzed using linear regression with RT BRE as the dependent variable and age as the independent factor. There was a significant positive effect

for age indicating older participants showed greater ratio sensitivity compared to younger participants, $r = .383$, $R^2 = .147$, $p = .010$. In order to evaluate age group differences, the RT BRE data were analyzed using a one-way ANOVA with age group as the between-subjects factor. There was a significant group effect, $F_{2, 41} = 3.415$, $\eta_P^2 = 0.143$, $p = .042$. Post-hoc contrasts using Least Significant Difference (LSD) tests showed that the RT BRE for adults was greater than that of children, $p = .013$. The BRE from adolescents did not differ significantly from either adults, $p = .175$, or children, $p = .242$. Thus, adults showed greater sensitivity to ratio effects compared to children, and adolescents indicated a transition period wherein ratio sensitivity fell between adults and children.

The right panel of Fig. 2 shows the mean accuracy for the total sample and each age group across the ratio bins and the mean accuracy BRE for each group. Accuracy increased monotonically from the lower more difficult ratios to the higher ratios. However, it is apparent from the data that ceiling effects may have limited the power of the linear regression to adequately characterize age effects. Mean accuracy for adults and adolescents in the two highest ratio bins and for children in the highest ratio bin were within one standard deviation of ceiling. One-sample *t*-tests showed that the mean accuracy for adults and adolescents in the *highest* ratio bin was not significantly below ceiling, and was not below ceiling in the *high* ratio bin for adolescents, *p*s ≥ .052. The mean performance for children across all ratio bins was significantly different from ceiling, *p*s ≤ .006. These performance levels were not unexpected as the test ratios were selected to optimally evaluate 10 year-old children. Consistent with the above, the full sample age effect was not significant, $r = .263$, $R^2 = .069$, $p = .085$. The group effect in the one-way ANOVA was not significant as well, $F_{2, 41} = 1.285$, $\eta_P^2 = 0.059$, $p = .288$. Despite the ceiling effect issues, the accuracy BRE for the entire sample and for each group separately were significantly above zero, indicating that the linear trend for accuracy was significant in all contrasts, *t*s ≥ 7.461, *p*s ≤ .001 (one-tailed), and the variance accounted for by the mean linear trends was reasonable: full sample $R^2 = .755$; adult $R^2 = .669$, adolescent $R^2 = .446$; child $R^2 = .792$. In summary, a significant BRE for accuracy was found in the full sample and in each age category signifying that accuracy was lowest for the lower ratio bin decisions and greatest for the highest ratio contrasts. However, ceiling effects precluded a reasonable comparison of differences related to age.

3.1.2 Math Achievement Effects—The relationship between the RT and accuracy BRE measures of numerosity acuity and math achievement scores are summarized in Figure 3 and Table II. In addition, Table I provides Pearson correlation coefficients for the relationship between age (natural logarithm), the Broad Math and individual subtest math achievement scores, together with the reading achievement (Letter-Word ID) and full scale IQ measures that were used as covariates in FMRI analysis. The analyses of the full sample and of each age group revealed no age-related differences across any of the standardized behavioral scores. Thus, achievement and IQ scores were well matched across the age spectrum in this sample.

Neither the RT or accuracy BRE measures proved to be significant predictors of math achievement. No significant relationship was found between the RT BRE and the main

Broad Math Index score, the four math achievement tests contributing to the Broad Math index, reading achievement, or full scale IQ, *p*s ≥ .326. Despite limitations in the reliability of the accuracy BRE related to ceiling effects (see above), the correlation findings between the accuracy BRE and all achievement measures were substantially similar to the RT BRE. In summary, neither measure of nonsymbolic numerosity acuity was found to be a reliable predictor of math academic achievement consistent with recent suggestions that nonsymbolic numerosity processes do not predict formal math achievement. Importantly, this includes formal math abilities in children.

3.2 FMRI Results

3.2.1 Motion and scrubbing results—There were no significant correlations (Pearson Correlation) with age in any of the three rotation or three translation axes (all $p_B > .05$). The number of censored volumes was not significantly related to age, $r = -.239$, $R^2 = .057$, $p = .118$. Overall, our strict inclusion criteria and scrubbing procedure resulted in minimal, well-matched motion across the age spectrum.

3.2.2 The Association between the Neural Ratio Effect (NRE), Age, and Math Achievement—A single repeated-measures ANCOVA was used to analyze age and math achievement effects together. Thus, the following results describe the independent contributions of each factor while controlling for the effects of the other (e.g., age controlling for math achievement). The dependent measure of math achievement is the omnibus Broad Math Index score from the Woodcock-Johnson III Tests of Achievement. Information regarding the correlations between the NRE measure and performance on each of the four math achievement subtests separately is provided in the Supplementary Information.

3.2.2.1 Age and the NRE: Figure 3 (left panel) and Table III describe the brain regions producing significant correlations between age (natural logarithm) and the NRE. Age effects were predominately positive, meaning the older participants produced a greater NRE than younger participants. Indeed, there were no negative effects observed in the parietal lobe. Positive parietal age effects included bilateral IPS, angular gyrus (BA 39), inferior parietal lobule including the supramarginal gyrus (BA 40), and the superior parietal lobule (BA 7). Positive age effects were also observed in the right hemisphere middle and inferior frontal gyri (BA 46/10 and 45, respectively). Negative NRE age effects, reflecting regions where ratio sensitivity was greater in younger participants relative to older participants were found largely in the left hemisphere including medial frontal cortical regions and lateral inferior frontal gyrus (BA 47). Overall, the parietal lobe areas produced the most extensive age effects for the NRE, showing increasing ratio sensitivity with development. These positive effects were generally more extensive in right hemisphere parietal cortex.

3.2.3.2 Math Achievement and the NRE: The math achievement effect on the NRE was evaluated using linear regression analysis with math achievement score as the continuous between-subjects variable. To control for overall cognitive ability and non-math academic achievement, FSIQ and a measure of reading achievement (Letter-Word Identification) were used as covariate factors. In addition, age was also included as a covariate. Achievement

data were unavailable for one child participant; thus, the linear analysis used data from 43 participants. Figure 3 (right panel) and Table 4 describe the brain activation results between math achievement and the NRE. Positive effects indicated that higher math achievement scores were associated with a greater NRE. Positive math achievement effects in parietal and frontal cortical regions were limited to the right hemisphere and included the IPS, superior parietal lobule (BA 7), inferior parietal lobule including the supramarginal gyrus (BA 40), and the precuneus (BA 7), together with activity in the superior aspects of the right middle and superior frontal gyri (BA 6 and 8/10, respectively). Positive achievement effects were also found in the posterior aspects of the VOT including bilateral lingual gyrus (BA 18) and cuneus (BA 17/18). Anterior VOT activity was limited to the right hemisphere anterior temporal pole (BA 21 and 38). In summary, across the entire developmental sample, right hemisphere positive effects between the NRE and math achievement tended to dominate the findings.

Although the above shows a positive trend between nonsymbolic ANS acuity and math achievement across the entire age sample, a significant question in the literature asks whether such an association can be observed specifically in children (see De Smedt, et al., 2013). To evaluate the association between math achievement and age with this question in mind, we analyzed data from children (6- to 12-years-old), adolescents (13- to 17-years-old), and adults (18-years and older) in separate regression analyses using age, FSIQ, and Letter-Word ID scores as covariates. Figure 4 and Table V describe these results. Pairwise contrasts used ANCOVA with math achievement as a continuous between-subjects factor and FSIQ and Letter-Word ID scores as covariates. Significant pairwise differences ($p < .05$) are denoted in Table 5. The striking finding was that only children produced a reliable positive math achievement effect in the IPS bilaterally. Children, but not adults or adolescents, produced extensive right parietal activity in addition to the IPS, including the regions of the SPL (BA 7), and the IPL including SMG (BA 40). Children also produced activation in the left hemisphere for these regions with the addition of the left angular gyrus (BA 39). Adults and children, but not adolescents, showed math achievement related activation within the left hemisphere IPL including the SMG. Therefore, higher individual scores on math achievement were associated with greater NRE responsiveness in right parietal cortex, but only in children. Children also activated homologous regions in the left hemisphere associated with math achievement. Adults and children produced robust positive activation within the VOT, especially in the right hemisphere, including the lingual gyrus, middle occipital gyrus, fusiform gyrus, middle temporal gyrus, and superior temporal gyrus. Interestingly, whereas children produced greater activation relative to adults in the most posterior aspects of the VOT, including the lingual and middle occipital gyrus (BA 18) and fusiform gyrus (BA 37), activation in adults was greater than children in the more anterior aspects of the VOT including the inferior, middle, and superior temporal gyri (BA 37/22. Thus, math achievement correlations to the NRE are found for both adults and children within the ventral visual processing stream, with children producing greater activation than adults primarily in extrastriate regions, and adults producing greater activation than children in the anterior processing regions. A surprising finding was that adults, but not children or adolescents, produced robust negative activation within the hippocampus bilaterally. That is,

poorer math achievement was associated with greater NRE sensitivity within the hippocampus for adults only.

4. Discussion

To the best of our knowledge, this is the first study of nonsymbolic numerosity to collect FMRI data spanning the age range from the school-age period into adulthood using continuous age range sampling paired with the collection of contemporaneous standardized academic achievement and IQ data. This allowed us to examine the links between nonsymbolic numerosity and math achievement using whole-brain regression analyses while controlling for age, non-math academic achievement, and overall cognitive abilities.

The behavioral findings from the nonsymbolic numerosity task proved two important points. First, reaction time and accuracy measures were sensitive to the parametric changes in dot ratios, a phenomenon here termed the behavioral ratio effect (BRE). Despite a ceiling effect in accuracy with the older participants in the higher ratio comparisons, accuracy was lower and reaction time longer across the age spectrum when responding to more difficult lower ratio problems compared to easier higher ratio problems. As expected, the BRE for younger participants indicated lower numerosity magnitude judgment acuity compared to older participants consistent with other studies (see Halberda, et al., 2012). The positive developmental trend between RT and BRE appears to contradict a previous study that included nonsymbolic magnitude contrasts that found adults produced a diminished distance effect relative to children (Holloway and Ansari, 2008). That is, the BRE for adults was less than the BRE observed for children. That study, however, used only magnitudes between 1 and 9 with numeric distances between the stimuli ranging from one to six (e.g., 3 squares vs. 9 squares, 5 squares vs. 6 squares). Thus, magnitudes within the subitizing range were included. Adults responded significantly faster than children at all distance levels, but RTs for adults were not provided. Thus, it is possible that their task was too easy for adults and did not induce sufficient variance in RTs across the distance variable to effectively evaluate a positive developmental trend. Our task used a broader range of magnitudes that afforded us the ability to observe significant variance across ratios in adults. Nevertheless, few studies have explicitly evaluated RT as the dependent variable for the BRE and more research is needed to confirm that the BRE continues to improve across development.

Most importantly for this study, RT and accuracy BRE measures did not reliably predict formal math achievement after controlling for overall cognitive ability and non-math (reading) achievement in the full sample, or in any of the three age groups evaluated separately. These behavioral results are consistent with the conclusion that nonsymbolic numerosity acuity does not in and of itself correlate significantly with formal math achievement. We note that our sample was primarily comprised of individuals that scored in the average range and above on all of the math and reading achievement and IQ measures. Thus, our sample of children (WJ Broad Math Index Scaled Score range: 81–141; mean = 112.4), adolescents (range: 82–147; mean = 111.2), and adults (range: 80–135; mean = 116.9) should be considered as comprised of typical through high math achieving individuals for their age, with participants spanning the qualitative “low average” to “superior” ranges (Sattler, 1992). Our findings stand in contrast to the influential study from

Halberda and colleagues (2008), where they found a measure of ANS acuity obtained in 9th grade children (14 years-old) significantly correlated with math achievement scores collected during Kindergarten through 6th grade (about 5 to 11 years old). That sample included children with achievement standard scores in the 60 to 80 point range (see Figures 2a and 2b, p. 666, Halberda, et al., 2008), falling qualitatively within the “borderline” to “impaired” ranges. It is possible that the inclusion of these lower achieving children increased the score range relative to our sample, and may account for the correlation between nonsymbolic numerosity acuity and formal math achievement. Also, the TEMA-2 measure used as one of two math measures in that study included test items that covered informal math knowledge in addition to formal math knowledge. A more recent study measuring behavioral nonsymbolic acuity on four separate occasions over two years in 3- to 7-year-old children found a reliable correlation only between informal math information on the TEMA-3 and not formal math material (Libertus, et al., 2013). Standard scores were not reported in that study. In summary, our behavioral findings demonstrate that behavioral nonsymbolic numerosity acuity does not appear to predict formal math achievement within typical and high achieving individuals in the age range we evaluated, a finding with growing acceptance in the field (De Smedt, et al., 2013; Libertus, et al., 2013).

Developmental changes in the neural foundations of nonsymbolic numerosity acuity were evaluated using a neural ratio effect (NRE), a BOLD signal equivalent of the BRE. Each individual’s NRE denoted the voxelwise parametric difference in BOLD activity based on the orthogonal linear effect of BOLD responses across the four ratio bins. A positive NRE indicated that the BOLD signal was maximal in response to the more difficult lower ratio magnitude problems relative to the easier higher ratio problems. As expected, we found significant positive NRE age effects in bilateral IPS, a region long associated with performance on numerosity tasks (Dehaene, et al., 2003), and consistent with an accumulating FMRI literature that neural ratio acuity in the IPS, be that for nonsymbolic or symbolic numerosity tasks, improves from childhood into adulthood (Ansari and Dhital, 2006; Cantlon, et al., 2006; Cantlon, et al., 2009a; Holloway and Ansari, 2010; Kaufmann, et al., 2008; Kovas, et al., 2009; Kucian, et al., 2008). Less expected was the broad activation of other parietal and frontal lobe areas. The parietal regions included bilateral inferior parietal lobule with the supramarginal gyrus, superior parietal lobule, angular gyrus, and precuneus. The frontal lobe areas included right hemisphere inferior and middle frontal gyri. These regions have been implicated as participating in many different aspects of mathematical cognition and show developmental effects. For example, activation of the right SPL has been observed during subtraction and multiplication operations (Arsalidou and Taylor, 2011), and has shown greater activation in adults compared to children (Kaufmann, et al., 2011). The left IPL and SMG show developmental trends with greater activation in adults compared to children during calculation tasks (Rivera, et al., 2005), and right IPL and SMG show a similar trend in magnitude comparison (Kucian, et al., 2008). Right hemisphere inferior and middle frontal gyrus regions have been identified as contributing to performance on tasks of multiplication and subtraction (Arsalidou and Taylor, 2011) and respond roughly equivalently on nonsymbolic and symbolic magnitude tasks (Holloway, et al., 2010). Nevertheless, developmental effects in the nonsymbolic NRE would not

necessarily be predicted within these regions when these various mathematical computations were not required during task performance.

We suggest that the NRE captures additional cognitive activity over and above that of the approximate number system per se. Specifically, the regional patterns of age-related changes in NRE suggest that the NRE is also sensitive to processes related to visuospatial processing, attention, and cognitive control. This is certainly the case for the bilateral activity within the superior parietal lobule areas and precuneus that were considered regions for attentional processing in the three parietal circuits model for number processing (Dehaene, et al., 2003). Attention effects extend also to the angular gyrus. For example, Gobel et al. (2001) applied repetitive transcranial magnetic stimulation (RTMS) to right and left hemisphere angular gyrus during a visuospatial search task with numbers. They found that the RTMS disruption of angular gyrus activity affected both visuospatial search functions and the typical organization of number sequencing (e.g., “number line”). The age effects in frontal lobe regions likely also signal compound effects. Right inferior frontal cortex regions play a role in cognitive control and inhibitory processes (Aron, et al., 2004; Aron, et al., 2014), and have an extended developmental trajectory (Davidson, et al., 2006). Within the context of the nonsymbolic numerosity task, these regions may become more responsive when magnitude decisions become more difficult and responses must be delayed to improve accuracy (i.e., speed-accuracy tradeoff), a factor that is more efficient in older participants. Specifically, top-down control guided by these frontal lobe areas may be less efficient in children compared to adults, a finding that has been established in language studies (Bitan, et al., 2006). In summary, we suggest that the NRE measure of nonsymbolic numerosity is a complex measure capturing aspects of magnitude estimation acuity in addition to visuospatial and cognitive control processes that together show extended developmental trajectories. The various cognitive components captured by the nonsymbolic NRE depend on a variety of cognitive brain circuits.

The central question of this study concerned the relationship between brain activity for nonsymbolic numerosity and math achievement across development. Unlike our behavioral results, the NRE measure was significantly positively correlated to math achievement. Correlated activity was observed within right hemisphere parietal cortex, including the IPS, superior parietal lobule, inferior parietal lobule including supramarginal gyrus, and precuneus. We observed no NRE effects in left hemisphere parietal regions. The analysis included age as a covariate in addition to using age-corrected scaled scores; hence, the overlap in regional activation in the age effect described above and math achievement represent independent contributions of the two effects. At first blush, the right parietal findings appear to provide the missing link indicating that functional BOLD nonsymbolic numerosity acuity can predict individual differences in formal math achievement noted as absent from the literature by De Smedt et al. (2013). However, their assertion specifically noted that no such data were available for typically developing children. Our full sample data conceivably could have been skewed by a dominant positive effect in adults and older adolescents with little or no correlation, or possibly even a negative correlation, between the NRE measure and individual math achievement in children. To evaluate this possibility, we conducted separate regression analyses in children (age 6 to 12 years), adolescents (13 to 17 years), and adults (≥18 years).

The separate group analyses provided evidence for a strong positive correlation between the NRE measure and math achievement within the IPS and surrounding parietal cortex bilaterally, but only in the child participants. With the exception of a positive correlation limited to the left precuneus in adults, neither the adults nor adolescents provided evidence for a reliable link between nonsymbolic acuity parietal activity and formal math achievement. Thus, the findings from the analysis of the full sample of participants appear to have been driven primarily by the association of achievement and NRE in children. An interesting aspect of the correlative activity in children is that although bilateral activation of IPS, inferior parietal lobule including supramarginal gyrus, superior parietal lobule, and angular gyrus were observed, the activation intensity and extent were generally greater in the left hemisphere (see Table V and Figure 4). The Woodcock-Johnson III Broad Math Index is comprised of scores from four subtests evaluating formal math knowledge and procedures via linguistic means including paper-and-pencil calculations using Arabic numerals (Calculation and Math Fluency subtests), visual and verbally presented word problems (Applied Problems), and visual and verbally presented mathematics knowledge questions (Quantitative Concepts). Therefore, the tasks are largely dependent on math symbolic and linguistic processing. Dehaene and colleagues (2011; 2003) describe an important role for left hemisphere parietal processing, particularly in regard to the superior parietal lobule and angular gyrus, for linguistic processing that participates in mathematical operations that place significant demands on verbal coding of numbers. It seems reasonable to suggest that even in children a left hemisphere bias might be related to the linguistic nature of the achievement tests. The important proviso is that such processing does not reliably support math achievement performance in adolescents and adults (Inglis, et al., 2011; Price, et al., 2012).

The role for nonsymbolic numerosity acuity in supporting formal math knowledge in children is not clear. Some suggest that this primitive math ability may support the mapping of quantity to number symbol meanings and the retrieval of such knowledge (De Smedt, et al., 2009; Holloway and Ansari, 2009). That is, nonsymbolic numerosity may provide the scaffolding for the transition between knowledge of numbers as quantities and magnitudes, and basic counting skills, to learning the association between quantities and Arabic numerals and formal expressions for addition, subtraction, and multiplication. On the other hand, correlations are agnostic regarding direction of causality. The children in our sample were exposed to a considerable level of formal math education as evidenced by their above average math achievement scores for their age. Perhaps formal math education acts to hone quantity estimates such that symbolic level math knowledge may boost the ability for quantity contrasts. As noted above in regard to the numerosity acuity aging effect, the areas observed as active in the NRE and math achievement correlation included regions that have strong ties to visuospatial attention, a cognitive domain that shows a strong correlation to math achievement in children in this age and high achievement range (Geary, 2011; Li and Geary, 2013). Tibber and colleagues (2013) reached a similar conclusion using psychophysical measurements across multiple domains in a developmental sample spanning ages from 6 to 73 years. They found that numerosity was not a unique predictor of mathematical ability, but was one of multiple visuospatial factors contributing to associations with math performance. As noted by Kaufmann et al. (2011), the present lack of

developmental data on numerical cognition limits our ability to specify the precise functional properties of these findings. Whatever the mechanism or mechanisms producing the NRE and math achievement correlation, the phenomenon is restricted to children.

The failure to find an association between nonsymbolic numerosity acuity and math achievement in the older participants in our sample (i.e., adolescents and adults) is consistent with mounting evidence from brain studies that such a relationship does not exist. A recent study using transcranial noise stimulation (TRNS) during nonsymbolic numerosity training in adults highlights the dissociation between brain functions supporting numerosity acuity and math proficiency. TRNS is a non-invasive stimulation technique applied at the scalp that modulates underlying cortical activity and can alter brain plasticity during cognitive training (Snowball, et al., 2013; Terney, et al., 2008). Cappelletti and colleagues (2013; see also Chick, 2014) applied TRNS to left and right parietal regions underlying the P3/P4 scalp areas derived from the International 10/20 system putatively affecting regions of the IPL, SPL, and IPS during nonsymbolic numerosity training. They found significant improvements in numerosity acuity after training. Interestingly, improvements extended to other magnitude judgments based on space and time discrimination that have also been linked to parietal lobe operations (Cantlon, et al., 2009b; Cohen Kadosh, et al., 2008b; Dormal, et al., 2012a; Dormal, et al., 2012b; Walsh, 2003), but not other cognitive functions such as attention, executive functions, and visual pattern recognition. Crucially, improved nonsymbolic numerosity acuity did not produce any concomitant improvement in arithmetical abilities.

A natural question to arise from our findings is why brain measures from children support a link between numerosity acuity and math achievement, whereas behavioral measures from RT and BRE do not? De Smedt et al. (2013) noted that behavioral studies of nonsymbolic numerosity have produced very inconsistent results, with about equal numbers of studies indicating a correlation and that fail to find a relationship (see also, Fazio, et al., 2014). The inconsistency in findings cut across tasks using RT, accuracy, and Weber fraction scores. It is not likely that these inconsistent findings were due to basic psychometric factors such as test unreliability. Maloney and colleagues (2010) evaluated the reliability of a nonsymbolic numerosity task and showed that both RT and accuracy measures were highly reliable. Indeed, they found that reliability of numeric distance effects for nonsymbolic tasks far exceeded those of symbolic tasks. However, De Smedt and colleagues indicated that symbolic numerosity tasks provided very consistent correlations between numerosity acuity and math achievement. It appears that the most reasonable conclusion to the difference in the brain and behavior correlations in our study is that our NRE brain measure is simply more sensitive than behavioral measures of nonsymbolic numerosity acuity, at least in children.

A very different developmental picture for the relationship between the nonsymbolic NRE and math achievement emerged in the ventral occipital and temporal (VOT) cortex. Here, we observed widespread and robust bilateral positive correlations in adults and children, but not in the adolescent group. Adults and children both produced positive correlations within bilateral lingual gyrus (BA 18), bilateral cuneus, and the left superior temporal gyrus (BA 22). Left superior temporal gyrus activity has been shown to increase during linguistic

analysis of mathematical syntax in algebra-style equations and hypothesized to indicate automatized visuospatial analysis of math syntax in accomplished math learners that reduces demands on the language system (Maruyama, et al., 2012). Cuneus activity has been observed in adults during magnitude estimation studies that required exact estimates for responses and was hypothesized to depend on visual memory matching strategies (Gandini, et al., 2008a). However, it is not clear how the NRE measured in our study taps into such processes to produce the correlations we observed, or how such activity could be observed in children that have not reach advanced levels of math knowledge. Potentially more significant than the limited overlap between adults and children are the differences in regional VOT activation. Children tended to produce significantly greater correlated activity relative to adults and adolescents in right hemisphere posterior VOT cortex, including right middle occipital gyrus (BA 18), right fusiform gyrus (BA 37), and right posterior middle temporal gyrus (BA 18). In contrast, adults produced greater correlated activity in the right superior temporal gyrus (BA 22), right anterior aspects of the middle temporal gyrus (BA 22), and left insula. Thus, the activity in children was focused within extrastriate cortex whereas adult activity was focused in cortical regions for higher order visual processing. The broad scale of VOT activation in response to the NRE is not surprising given the accumulating evidence from behavioral and EEG studies suggesting that magnitude estimation performance may be supported by visual discrimination of subtle differences in the properties of nonsymbolic numerosity stimuli rather than numerosity acuity per se (Gebuis and Reynvoet, 2012a; Gebuis and Reynvoet, 2012b; Gebuis and Reynvoet, 2012c; Gebuis and Reynvoet, 2013). Our findings suggest that the acuity of those visual discrimination processes positively correlate to math academic achievement, but also suggest that children rely on different aspects of visual discrimination compared to adults who show greater reliance on higher order visual processing capabilities.

One important conclusion drawn from these developmental findings is that the VOT correlations between the NRE and math achievement suggests a dynamic process of reorganization of functions from childhood through adulthood. Specifically, regional overlap in activation between adults and children was limited. Our linear regression analysis controlling for age found a consistent correlation in the posterior VOT regions only in the bilateral lingual gyrus, cuneus, right middle occipital gyrus, and posterior interior temporal gyrus (see Table 4 and Figure 3). Yet, the critical qualification to these findings is that we found no reliable positive correlations between NRE and math achievement in our adolescent group. Thus, an apparent link between visuospatial-based nonsymbolic magnitude estimation acuity and math achievement breaks down during this dynamic developmental period. This supports the realistic possibility that the precise mechanisms supporting the positive correlations in children differ significantly from those observed in adults. No functional imaging studies to date have specifically evaluated differences in visuospatial mechanisms in numerosity tasks across development. Such work is needed to define the transition in sensory, perceptual, and cognitive changes that occur between the childhood and adolescent period in which significant advances in mathematical knowledge are expected.

A surprising finding in adults was the strong negative correlation between the NRE and math achievement in the hippocampus bilaterally with a right hemisphere bias in the extent

and intensity of the FMRI signal. Examination of the correlation between the adult NRE and achievement on the individual subtests of the Woodcock-Johnson test suggest that performance on the Math Fluency subtest, a timed measure of addition, subtraction, and multiplication using digits between 1 and 10, predominately drove this negative hippocampal correlation (see Supplementary Information). The functions of the hippocampus are most closely associated with declarative memory functions (Eichenbaum, 2004; Squire, et al., 2004). Some models of numerosity performance include a role for retrieval functions from memory (Gandini, et al., 2008b) or Hebbian associative functions for which the hippocampus may participate (Dehaene and Changeux, 1993). In adults, using strategies based on such models are generally considered more efficient compared to alternative strategies, particularly when numerosity judgments must be translated into more precise exact estimates (Gandini, et al., 2008a). As our study did not require translation to exact numeric estimates, we suggest a possible alternative explanation. Evidence from neuroimaging and human lesion studies point to an important role for the medial temporal lobe in visual discrimination for stimuli that cannot be distinguished easily by differences in shape information (Barense, et al., 2005; Bussey and Saksida, 2007; Graham, et al., 2010; Lee, et al., 2012; O'Neil, et al., 2009). The medial temporal lobe receives the most highly processed visual information from the ventral visual pathway (Kravitz, et al., 2013; Ungerleider and Mishkin, 1982; Van Essen, et al., 1992). Recent evidence also points to the medial temporal lobe receiving direct and indirect input from posterior parietal cortex of the dorsal "where" or "what" pathway, including the IPS region (Kravitz, et al., 2011). This places the medial temporal lobe in the position to associate numerosity information both from high-level visual discrimination processes available through the ventral visual processing stream and visuospatial processes dependent on parietal lobe functions. In adults, nonsymbolic numerosity acuity in "earlier" stages of ventral visual processing stream was positively correlated with math achievement. We use the term "earlier" cautiously noting evidence that information processing within this stream is not organized in a serial fashion, but depends crucially on bottom-up and top-down information processing (Kravitz, et al., 2013). If one views the pattern of correlations to math achievement as a marker of the integrity of visual discrimination processing, an efficient system is capable of resolving nonsymbolic magnitude estimation contrasts earlier in the processing stream. Using the young adults in this sample to represent the "peak stage" of the developmental process, the findings suggest that individuals with less efficient visual discrimination abilities that require discrimination based on the highest-order functions acquired relatively less formal math knowledge. Conversely, those individuals capable of resolving more difficult nonsymbolic magnitude estimation problems using visual processing areas earlier in the processing stream acquired relatively more formal math knowledge. Thus, we suggest the efficiency of neural visual discrimination for magnitude judgments is associated with the capacity to acquire formal math knowledge.

5. Conclusions

Nonsymbolic numerosity, or the basic sense of numbers, is an evolutionarily old skill that humans share with many other species. The role of this ability in supporting the acquisition and use of formal mathematics knowledge across development is a question of fundamental

importance in cognitive and educational neuroscience. Our study produced three significant findings. Consistent with accumulating evidence, behavioral measures of nonsymbolic numerosity proved to be poor predictors of formal math knowledge acquisition as measured by academic achievement tests. Such was not the case with brain activation measures of nonsymbolic numerosity acuity. Our FMRI findings from a continuous age sample spanning school age children through adults showed that brain activation for greater numerosity acuity in the parietal lobe was positively correlated to math academic achievement in children, but not in adolescents or adults. These findings provide the first definitive evidence for an association between nonsymbolic numerosity skills and the acquisition of formal math knowledge in development (De Smedt, et al., 2013). While the precise nature or directionality of these effects in children remain open for study, these data contribute to a growing literature suggesting nonsymbolic numerosity skill does not provide significant support for higher-level math knowledge, such as that used in algebra, geometry, and calculus. We observed a significant developmental transition in the relationship of nonsymbolic numerosity acuity to math achievement within the ventral visual processing stream. Of note, children and adults produced significant positive correlations to math achievement in distinct areas within the ventral stream. Taken together with null findings from adolescents, the findings suggest a dynamic developmental process occurring from school age to young adulthood in visual discrimination strategies that predict the acquisition of formal math knowledge. Moreover, a negative correlation between math achievement and nonsymbolic numerosity acuity in the hippocampus in adults suggest that the efficiency of visual discrimination strategies has profound implications for the acquisition of formal math knowledge during development.

Supplementary Material

Refer to Web version on PubMed Central for supplementary material.

Acknowledgments

Contract grant sponsor: National Institute of Child Health and Human Development

Contract grant number: R24 HD075489

We thank Natacha Akshoomoff, Joan Stiles, Terry Jernigan, and two anonymous reviewers for helpful comments on the manuscript, Mehdi Bouhaddou, Jason Meng, Shelley Kuang, Jessie Rosales, and Amy Shipow for assistance with data collection and analysis, and B. H. Akshoomoff for assistance with manuscript preparation.

Abbreviations

ANS	approximate number system
IPS	intraparietal sulcus
IPL	inferior parietal lobule
SPL	superior parietal lobule
BA	Brodmann’s area
NRE	neural ratio effect

BRE behavioral ratio effect

ROI region(s) of interest

References

Agrillo C. Once upon a time there was complex numerical estimation. Front Hum Neurosci. 2012; 6:300. [PubMed: 23133412]

Ansari D. Effects of development and enculturation on number representation in the brain. Nat Rev Neurosci England. 2008:278–91.

Ansari D, Dhital B. Age-related changes in the activation of the intraparietal sulcus during nonsymbolic magnitude processing: an event-related functional magnetic resonance imaging study. J Cogn Neurosci. 2006; 18:1820–8. [PubMed: 17069473]

Aron AR, Robbins TW, Poldrack RA. Inhibition and the right inferior frontal cortex. Trends Cogn Sci England. 2004:170–7.

Aron AR, Robbins TW, Poldrack RA. Inhibition and the right inferior frontal cortex: one decade on. Trends Cogn Sci. 2014; 18:177–85. [PubMed: 24440116]

Arsalidou M, Taylor MJ. Is 2+2=4? Meta-analyses of brain areas needed for numbers and calculations. Neuroimage. 2011; 54:2382–93. [PubMed: 20946958]

Barense MD, Bussey TJ, Lee AC, Rogers TT, Davies RR, Saksida LM, Murray EA, Graham KS. Functional specialization in the human medial temporal lobe. J Neurosci. 2005; 25:10239–46. [PubMed: 16267231]

Beauchamp MS. Detection of eye movements from fMRI data. Magn Reson Med. 2003; 49:376–80. [PubMed: 12541259]

Beckmann CF, Smith SM. Probabilistic independent component analysis for functional magnetic resonance imaging. IEEE Trans Med Imaging. 2004; 23:137–52. [PubMed: 14964560]

Bitan T, Burman DD, Lu D, Cone NE, Gitelman DR, Mesulam MM, Booth JR. Weaker top-down modulation from the left inferior frontal gyrus in children. Neuroimage. 2006; 33:991–998. [PubMed: 16978881]

Brannon EM. The representation of numerical magnitude. Curr Opin Neurobiol. 2006; 16:222–9. [PubMed: 16546373]

Bugden S, Price GR, McLean DA, Ansari D. The role of the left intraparietal sulcus in the relationship between symbolic number processing and children's arithmetic competence. Dev Cogn Neurosci. 2012; 2:448–57. [PubMed: 22591861]

Bussey TJ, Saksida LM. Memory, perception, and the ventral visual-perirhinal-hippocampal stream: thinking outside of the boxes. Hippocampus. 2007; 17:898–908. [PubMed: 17636546]

Butterworth B, Walsh V. Neural basis of mathematical cognition. Curr Biol. 2011; 21:R618–21. [PubMed: 21854998]

Cantlon JF. Math, monkeys, and the developing brain. Proc Natl Acad Sci U S A. 2012; 109(Suppl 1): 10725–32. [PubMed: 22723349]

Cantlon JF, Brannon EM, Carter EJ, Pelphrey KA. Functional imaging of numerical processing in adults and 4-y-old children. PLoS Biol. 2006; 4:e125. [PubMed: 16594732]

Cantlon JF, Libertus ME, Pinel P, Dehaene S, Brannon EM, Pelphrey KA. The neural development of an abstract concept of number. J Cogn Neurosci. 2009a; 21:2217–29. [PubMed: 19016605]

Cantlon JF, Platt ML, Brannon EM. Beyond the number domain. Trends Cogn Sci. 2009b; 13:83–91. [PubMed: 19131268]

Cappelletti M, Gessaroli E, Hithersay R, Mitolo M, Didino D, Kanai R, Cohen Kadosh R, Walsh V. Transfer of cognitive training across magnitude dimensions achieved with concurrent brain stimulation of the parietal lobe. J Neurosci. 2013; 33:14899–907. [PubMed: 24027289]

Castronovo J, Gobel SM. Impact of high mathematics education on the number sense. PLoS One. 2012; 7:e33832. [PubMed: 22558077]

Chick CF. Basic mechanisms of numerical processing: cross-modal number comparisons and symbolic versus nonsymbolic numerosity in the intraparietal sulcus. J Neurosci. 2014; 34:1567–9. [PubMed: 24478340]

Choo H, Franconeri SL. Enumeration of small collections violates Weber's law. Psychon Bull Rev. 2014; 21:93–99. [PubMed: 23824632]

Cohen Kadosh R, Cohen Kadosh K, Henik A. When brightness counts: the neuronal correlate of numerical-luminance interference. Cereb Cortex. 2008a; 18:337–43. [PubMed: 17556772]

Cohen Kadosh R, Cohen Kadosh K, Kaas A, Henik A, Goebel R. Notation-dependent and -independent representations of numbers in the parietal lobes. Neuron. 2007; 53:307–14. [PubMed: 17224410]

Cohen Kadosh R, Lammertyn J, Izard V. Are numbers special? An overview of chronometric, neuroimaging, developmental and comparative studies of magnitude representation. Prog Neurobiol. 2008b; 84:132–47. [PubMed: 18155348]

Cohen MS. Parametric analysis of fMRI data using linear systems methods. Neuroimage. 1997; 6:93–103. [PubMed: 9299383]

Cox RW, Hyde JS. Software tools for analysis and visualization of fMRI data. NMR Biomed. 1997; 10:171–8. [PubMed: 9430344]

Davidson MC, Amso D, Anderson LC, Diamond A. Development of cognitive control and executive functions from 4 to 13 years: evidence from manipulations of memory, inhibition, and task switching. Neuropsychologia. 2006; 44:2037–78. [PubMed: 16580701]

de Hevia MD, Girelli L, Bricolo E, Vallar G. The representational space of numerical magnitude: illusions of length. Q J Exp Psychol. 2008; 61:1496–514.

De Smedt B, Noël MP, Gilmore C, Ansari D. How do symbolic and non-symbolic numerical magnitude processing skills relate to individual differences in children's mathematical skills? A review of evidence from brain and behavior. Trends in Neuroscience and Education. 2013; 2:48–55.

De Smedt B, Verschaffel L, Ghesquiere P. The predictive value of numerical magnitude comparison for individual differences in mathematics achievement. J Exp Child Psychol. 2009; 103:469–79. [PubMed: 19285682]

Dehaene S. Varieties of numerical abilities. Cognition. 1992; 44:1–42. [PubMed: 1511583]

Dehaene, S. The Number Sense: How the Mind Creates Mathematics, Revised and Updated Edition. New York, NY: Oxford University Press; 2011.

Dehaene S, Changeux JP. Development of elementary numerical abilities: a neuronal model. J Cogn Neurosci. 1993; 5:390–407. [PubMed: 23964915]

Dehaene S, Piazza M, Pinel P, Cohen L. Three parietal circuits for number processing. Cogn Neuropsychol. 2003; 20:487–506. [PubMed: 20957581]

Dormal V, Andres M, Pesenti M. Contribution of the right intraparietal sulcus to numerosity and length processing: an fMRI-guided TMS study. Cortex. 2012a; 48:623–9. [PubMed: 21722888]

Dormal V, Dormal G, Joassin F, Pesenti M. A common right fronto-parietal network for numerosity and duration processing: an fMRI study. Hum Brain Mapp. 2012b; 33:1490–501. [PubMed: 21692143]

Eichenbaum H. Hippocampus: cognitive processes and neural representations that underlie declarative memory. Neuron. 2004; 44:109–20. [PubMed: 15450164]

Fazio LK, Bailey DH, Thompson CA, Siegler RS. Relations of different types of numerical magnitude representations to each other and to mathematics achievement. J Exp Child Psychol. 2014; 123:53–72. [PubMed: 24699178]

Fisher RA. On a distribution yielding the error functions of several well known statistics. Proceedings of the International Congress of Mathematics, Toronto. 1924; 2:805–813.

Forman SD, Cohen JD, Fitzgerald M, Eddy WF, Mintun MA, Noll DC. Improved Assessment of Significant Activation in Functional Magnetic-Resonance-Imaging (FMRI) - Use of a Cluster-Size Threshold. Magn Reson Med. 1995; 33:636–647. [PubMed: 7596267]

Gandini D, Lemaire P, Anton JL, Nazarian B. Neural correlates of approximate quantification strategies in young and older adults: an fMRI study. Brain Res. 2008a; 1246:144–57. [PubMed: 18976641]

Gandini D, Lemaire P, Dufau S. Older and younger adults' strategies in approximate quantification. Acta Psychol (Amst). 2008b; 129:175–89. [PubMed: 18606394]

Geary DC. Cognitive predictors of achievement growth in mathematics: a 5-year longitudinal study. Dev Psychol. 2011; 47:1539–52. [PubMed: 21942667]

Gebuis T, Reynvoet B. Continuous visual properties explain neural responses to nonsymbolic number. Psychophysiology. 2012a; 49:1481–91. [PubMed: 23046492]

Gebuis T, Reynvoet B. The interplay between nonsymbolic number and its continuous visual properties. J Exp Psychol Gen. 2012b; 141:642–8. [PubMed: 22082115]

Gebuis T, Reynvoet B. The role of visual information in numerosity estimation. PLoS One. 2012c; 7:e37426. [PubMed: 22616007]

Gebuis T, Reynvoet B. The neural mechanisms underlying passive and active processing of numerosity. Neuroimage. 2013; 70:301–7. [PubMed: 23282277]

Gobel S, Walsh V, Rushworth MF. The mental number line and the human angular gyrus. Neuroimage. 2001; 14:1278–89. [PubMed: 11707084]

Gordon P. Numerical cognition without words: evidence from Amazonia. Science. 2004; 306:496–9. [PubMed: 15319490]

Graham KS, Barense MD, Lee AC. Going beyond LTM in the MTL: a synthesis of neuropsychological and neuroimaging findings on the role of the medial temporal lobe in memory and perception. Neuropsychologia. 2010; 48:831–53. [PubMed: 20074580]

Haist F, Adamo M, Han Wazny J, Lee K, Stiles J. The functional architecture for face-processing expertise: FMRI evidence of the developmental trajectory of the core and the extended face systems. Neuropsychologia. 2013; 51:2893–908. [PubMed: 23948645]

Haist F, Adamo M, Westerfield M, Courchesne E, Townsend J. The functional neuroanatomy of spatial attention in autism spectrum disorder. Dev Neuropsychol. 2005; 27:425–58. [PubMed: 15843105]

Halberda J, Feigenson L. Developmental change in the acuity of the "Number Sense": The Approximate Number System in 3-, 4-, 5-, and 6-year-olds and adults. Dev Psychol. 2008; 44:1457–65. [PubMed: 18793076]

Halberda J, Ly R, Wilmer JB, Naiman DQ, Germine L. Number sense across the lifespan as revealed by a massive Internet-based sample. Proc Natl Acad Sci U S A. 2012

Halberda J, Mazzocco MM, Feigenson L. Individual differences in non-verbal number acuity correlate with maths achievement. Nature. 2008; 455:665–8. [PubMed: 18776888]

Henik A, Leibovich T, Naparstek S, Diesendruck L, Rubinsten O. Quantities, amounts, and the numerical core system. Front Hum Neurosci. 2011; 5:186. [PubMed: 22319484]

Holloway ID, Ansari D. Domain-specific and domain-general changes in children's development of number comparison. Dev Sci England. 2008:644–9.

Holloway ID, Ansari D. Mapping numerical magnitudes onto symbols: the numerical distance effect and individual differences in children's mathematics achievement. J Exp Child Psychol United States. 2009:17–29.

Holloway ID, Ansari D. Developmental specialization in the right intraparietal sulcus for the abstract representation of numerical magnitude. J Cogn Neurosci. 2010; 22:2627–37. [PubMed: 19929327]

Holloway ID, Price GR, Ansari D. Common and segregated neural pathways for the processing of symbolic and nonsymbolic numerical magnitude: an fMRI study. Neuroimage. 2010; 49:1006–17. [PubMed: 19666127]

Holmes CJ, Hoge R, Collins L, Woods R, Toga AW, Evans AC. Enhancement of MR images using registration for signal averaging. J Comput Assist Tomogr. 1998; 22:324–33. [PubMed: 9530404]

Hyde DC. Two systems of non-symbolic numerical cognition. Front Hum Neurosci. 2011; 5:150. [PubMed: 22144955]

Inglis M, Attridge N, Batchelor S, Gilmore C. Non-verbal number acuity correlates with symbolic mathematics achievement: but only in children. Psychon Bull Rev. 2011; 18:1222–9. [PubMed: 21898191]

Kaufman EL, Lord MW. The discrimination of visual number. Am J Psychol. 1949; 62:498–525. [PubMed: 15392567]

Kaufmann L, Vogel SE, Wood G, Kremser C, Schocke M, Zimmerhackl LB, Koten JW. A developmental fMRI study of nonsymbolic numerical and spatial processing. Cortex. 2008; 44:376–85. [PubMed: 18387568]

Kaufmann L, Wood G, Rubinsten O, Henik A. Meta-analyses of developmental fMRI studies investigating typical and atypical trajectories of number processing and calculation. Dev Neuropsychol. 2011; 36:763–87. [PubMed: 21761997]

Kovas Y, Giampietro V, Viding E, Ng V, Brammer M, Barker GJ, Happe FG, Plomin R. Brain correlates of non-symbolic numerosity estimation in low and high mathematical ability children. PLoS One. 2009; 4:e4587. [PubMed: 19238205]

Kravitz DJ, Saleem KS, Baker CI, Mishkin M. A new neural framework for visuospatial processing. Nat Rev Neurosci. 2011; 12:217–30. [PubMed: 21415848]

Kravitz DJ, Saleem KS, Baker CI, Ungerleider LG, Mishkin M. The ventral visual pathway: an expanded neural framework for the processing of object quality. Trends Cogn Sci. 2013; 17:26–49. [PubMed: 23265839]

Kucian K, von Aster M, Loenneker T, Dietrich T, Martin E. Development of neural networks for exact and approximate calculation: a FMRI study. Dev Neuropsychol. 2008; 33:447–73. [PubMed: 18568899]

Laird AR, Robinson JL, McMillan KM, Tordesillas-Gutierrez D, Moran ST, Gonzales SM, Ray KL, Franklin C, Glahn DC, Fox PT, Lancaster JL. Comparison of the disparity between Talairach and MNI coordinates in functional neuroimaging data: validation of the Lancaster transform. Neuroimage. 2010; 51:677–83. [PubMed: 20197097]

Lancaster JL, Tordesillas-Gutierrez D, Martinez M, Salinas F, Evans A, Zilles K, Mazziotta JC, Fox PT. Bias between MNI and Talairach coordinates analyzed using the ICBM-152 brain template. Hum Brain Mapp. 2007; 28:1194–205. [PubMed: 17266101]

Lee AC, Yeung LK, Barense MD. The hippocampus and visual perception. Front Hum Neurosci. 2012; 6:91. [PubMed: 22529794]

Li Y, Geary DC. Developmental gains in visuospatial memory predict gains in mathematics achievement. PLoS One. 2013; 8:e70160. [PubMed: 23936154]

Libertus ME, Feigenson L, Halberda J. Preschool acuity of the approximate number system correlates with school math ability. Dev Sci. 2011; 14:1292–300. [PubMed: 22010889]

Libertus ME, Feigenson L, Halberda J. Numerical approximation abilities correlate with and predict informal but not formal mathematics abilities. J Exp Child Psychol. 2013; 116:829–38. [PubMed: 24076381]

Libertus ME, Odic D, Halberda J. Intuitive sense of number correlates with math scores on college-entrance examination. Acta Psychol (Amst). 2012; 141:373–9. [PubMed: 23098904]

Libertus ME, Woldorff MG, Brannon EM. Electrophysiological evidence for notation independence in numerical processing. Behavioral and brain functions: BBF. 2007; 3:1. [PubMed: 17214890]

Maloney, EA.; Risko, EF.; Preston, F.; Ansari, D.; Fugelsang, J. Acta Psychol (Amst). Vol. 2010. Netherlands: Elsevier B.V; 2010. Challenging the reliability and validity of cognitive measures: the case of the numerical distance effect; p. 154-161.

Maruyama M, Pallier C, Jobert A, Sigman M, Dehaene S. The cortical representation of simple mathematical expressions. Neuroimage. 2012; 61:1444–60. [PubMed: 22521479]

Mazzocco MM, Feigenson L, Halberda J. Preschoolers' precision of the approximate number system predicts later school mathematics performance. PLoS One. 2011; 6:e23749. [PubMed: 21935362]

McCrink K, Wynn K. Ratio abstraction by 6-month-old infants. Psychol Sci. 2007; 18:740–5. [PubMed: 17680947]

Neter, J.; Kutner, MH.; Nachtsheim, CJ.; Wasserman, W. Applied Linear Statistical Models. Boston, MA: WCB McGraw-Hill; 1996.

Nieder A. Coding of abstract quantity by 'number neurons' of the primate brain. J Comp Physiol A Neuroethol Sens Neural Behav Physiol. 2013; 199:1–16. [PubMed: 23052854]

Nieder A, Dehaene S. Representation of number in the brain. Annu Rev Neurosci. 2009; 32:185–208. [PubMed: 19400715]

O'Neil EB, Cate AD, Kohler S. Perirhinal cortex contributes to accuracy in recognition memory and perceptual discriminations. J Neurosci. 2009; 29:8329–34. [PubMed: 19571124]

Odic D, Hock H, Halberda J. Hysteresis affects approximate number discrimination in young children. J Exp Psychol Gen. 2014; 143:255–65. [PubMed: 23163765]

Oldfield RC. The assessment and analysis of handedness: The Edinburgh inventory. Neuropsychologia. 1971; 9:97–113. [PubMed: 5146491]

Perlbarg V, Bellec P, Anton JL, Pelegrini-Issac M, Doyon J, Benali H. CORSICA: correction of structured noise in fMRI by automatic identification of ICA components. Magn Reson Imaging. 2007; 25:35–46. [PubMed: 17222713]

Piazza M, Pinel P, Le Bihan D, Dehaene S. A magnitude code common to numerosities and number symbols in human intraparietal cortex. Neuron. 2007; 53:293–305. [PubMed: 17224409]

Pinel P, Dehaene S, Riviere D, LeBihan D. Modulation of parietal activation by semantic distance in a number comparison task. Neuroimage. 2001; 14:1013–26. [PubMed: 11697933]

Price GR, Mazzocco MM, Ansari D. Why mental arithmetic counts: brain activation during single digit arithmetic predicts high school math scores. J Neurosci. 2013; 33:156–63. [PubMed: 23283330]

Price GR, Palmer D, Battista C, Ansari D. Nonsymbolic numerical magnitude comparison: reliability and validity of different task variants and outcome measures, and their relationship to arithmetic achievement in adults. Acta Psychol (Amst). 2012; 140:50–7. [PubMed: 22445770]

Rivera SM, Reiss AL, Eckert MA, Menon V. Developmental changes in mental arithmetic: evidence for increased functional specialization in the left inferior parietal cortex. Cereb Cortex. 2005; 15:1779–90. [PubMed: 15716474]

Roitman JD, Brannon EM, Platt ML. Representation of numerosity in posterior parietal cortex. Front Integr Neurosci. 2012; 6:25. [PubMed: 22666194]

Sasanguie D, Gobel SM, Moll K, Smets K, Reynvoet B. Approximate number sense, symbolic number processing, or number-space mappings: what underlies mathematics achievement? J Exp Child Psychol. 2013; 114:418–31. [PubMed: 23270796]

Sattler, JM. Assessment of Children. San Diego, CA: Jerome M. Sattler, Publisher Inc; 1992.

Siegel JS, Power JD, Dubis JW, Vogel AC, Church JA, Schlaggar BL, Petersen SE. Statistical improvements in functional magnetic resonance imaging analyses produced by censoring high-motion data points. Hum Brain Mapp. 2014; 35:1981–1996. [PubMed: 23861343]

Simon TJ, Vaishnavi S. Subitizing and counting depend on different attentional mechanisms: Evidence from visual enumeration in afterimages. Percept Psychophys. 1996; 58:915–926. [PubMed: 8768186]

Snowball A, Tachtsidis I, Popescu T, Thompson J, Delazer M, Zamarian L, Zhu T, Cohen Kadosh R. Long-term enhancement of brain function and cognition using cognitive training and brain stimulation. Curr Biol. 2013; 23:987–92. [PubMed: 23684971]

Spaepen E, Coppola M, Spelke ES, Carey SE, Goldin-Meadow S. Number without a language model. Proc Natl Acad Sci U S A. 2011; 108:3163–8. [PubMed: 21300893]

Squire LR, Stark CE, Clark RE. The medial temporal lobe. Annu Rev Neurosci. 2004; 27:279–306. [PubMed: 15217334]

Talairach, J.; Tournoux, P. Co-planar Stereotaxic Atlas of the Human Brain. New York: Thieme Medical; 1988.

Terney D, Chaieb L, Moliadze V, Antal A, Paulus W. Increasing human brain excitability by transcranial high-frequency random noise stimulation. J Neurosci. 2008; 28:14147–55. [PubMed: 19109497]

Thomas MS, Annaz D, Ansari D, Scerif G, Jarrold C, Karmiloff-Smith A. Using developmental trajectories to understand developmental disorders. J Speech Lang Hear Res. 2009; 52:336–58. [PubMed: 19252129]

Tibber MS, Manasseh GS, Clarke RC, Gagin G, Swanbeck SN, Butterworth B, Lotto RB, Dakin SC. Sensitivity to numerosity is not a unique visuospatial psychophysical predictor of mathematical ability. Vision Res. 2013; 89:1–9. [PubMed: 23820087]

Tregellas JR, Tanabe JL, Miller DE, Freedman R. Monitoring eye movements during fMRI tasks with echo planar images. Hum Brain Mapp. 2002; 17:237–243. [PubMed: 12395391]

Ungerleider, LG.; Mishkin, M. Two cortical visual systems. In: Ingle, DJ.; Goodale, MA.; Mansfield, RJW., editors. Analysis of visual behavior. Cambridge, MA: The MIT Press; 1982. p. 549-586.

Van Essen DC, Anderson CH, Felleman DJ. Information processing in the primate visual system: an integrated systems perspective. Science. 1992; 255:419–23. [PubMed: 1734518]

Walsh V. A theory of magnitude: common cortical metrics of time, space and quantity. Trends Cogn Sci. 2003; 7:483–8. [PubMed: 14585444]

Wechsler, D. Wechsler Abbreviated Scale of Intelligence Manual. New York: The Psychological Corporation; 1999.

Woodcock, RW.; McGrew, KS.; Mather, N. Woodcock-Johnson III Normative Update Tests of Achievement. Rolling Meadows, IL: Riverside Publishing Co; 2007.

Xu F, Spelke ES. Large number discrimination in 6-month-old infants. Cognition. 2000; 74:B1–B11. [PubMed: 10594312]

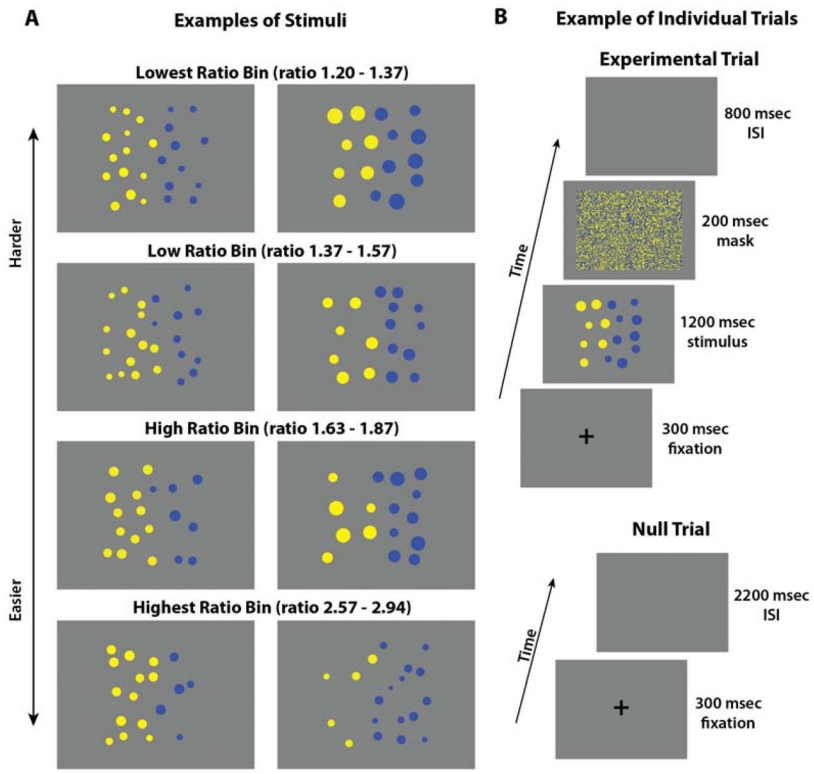

Figure 1.

The nonsymbolic numerosity task used a randomized event-related fMRI design presented in two counterbalanced runs. (A) Examples of stimuli, categorized into four “ratio bins” with a continuous set of ratios within a range. A ratio is defined as the greater value divided by the smaller value (i.e., 6 dots/5 dots = ratio of 1.2). Participants were instructed to press one of two buttons to indicate which cloud of colored dots contained the greater number of dots. The experimental stimuli consisted of yellow dots on the left side of the screen (RGB = 255/255/0) and blue dots on the right side (RGB = 0/0/255) against a gray background (RGB = 128/128/128). (B) Example of a series of experimental and null trials. The order of presentation of stimulus and null trials was pseudorandomized.

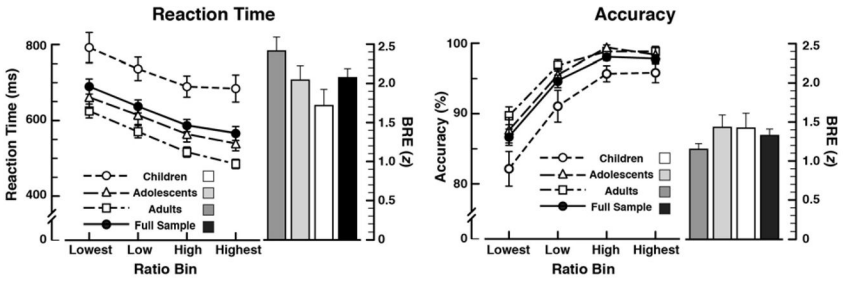

Figure 2.

Behavioral results of the individual participants from the nonsymbolic numerosity task. (A) Regressions by age (natural logarithm) with accuracy (percent correct), reaction time (RT; in ms) shown in left and right panels, respectively. Accuracy was poorer in younger compared to older participants. Linear effects of age were not equivalent across ratio ranges, with the slope of the low ratio bin significantly more positive than the high and highest bins. Of note, there were ceiling levels of performance in the high and highest ratio bins for each of the age groups, most likely due to the task using ratios that were optimized for 10-year olds. There was a clear BRE in the lowest and low ratios, whereupon accuracy was lowest and the age-effects were maximally observed. The RT to make correct response significantly decreased as age increased. (B) Regressions for accuracy and RT by math achievement. Math achievement was not a strong predictor of accuracy or RT performance on the numerosity task.

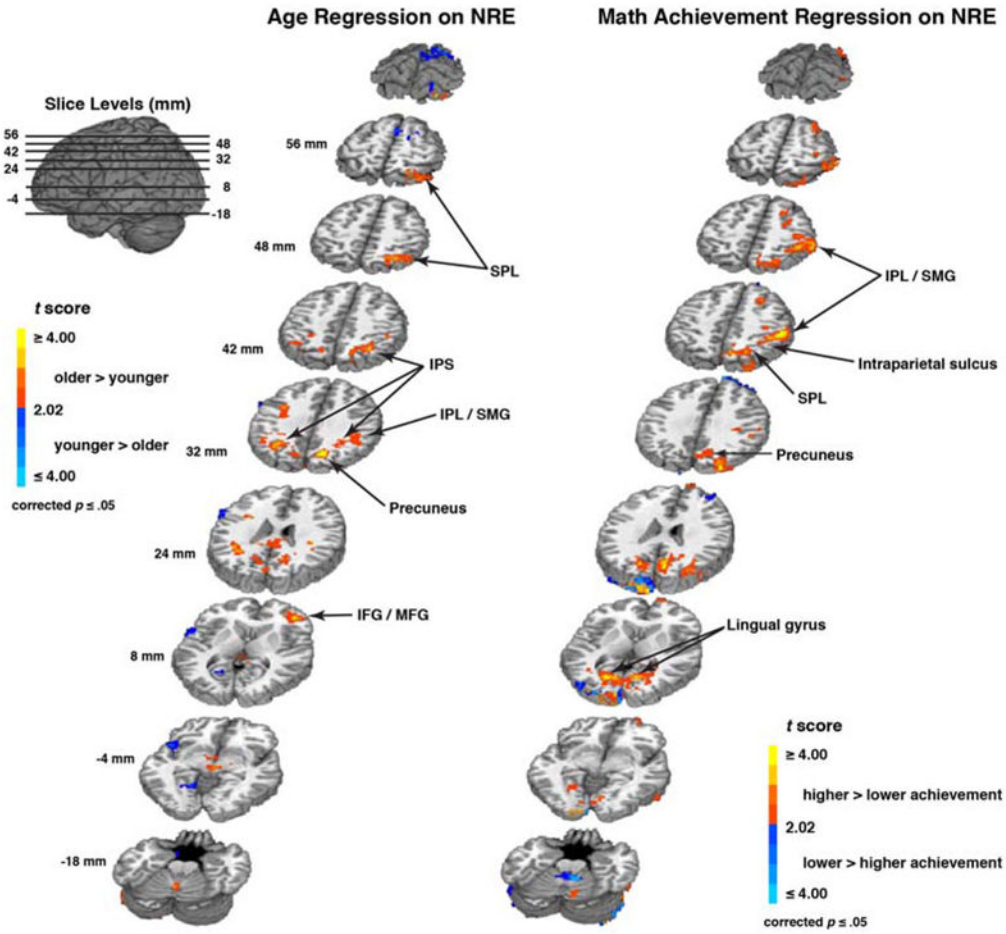

Figure 3.

Brain regions producing significant age effects and math achievement effects from the regression analyses against the neural ratio effect (NRE). (Left panel) Regions showing significant age (natural logarithm in years) effects against the NRE. Warm colors show regions where age was positively correlated to nonsymbolic numerosity acuity as measured by the NRE, and cooler colors where age was negatively correlated to the NRE. Regions in parietal cortex, including the intraparietal sulcus (IPS), SPL, IPL, and precuneus, produced positive developmental age effects. Overall, right hemisphere activity was greater than left hemisphere activity. A complete description of regional activation is provided in Table III. (Right panel) Regions showing significant math achievement effects against the NRE. Warm colors show regions where higher math achievement scores were positively correlated to the NRE, and cooler colors where math achievement was negatively correlated to the NRE. Regions in parietal cortex, including the IPS, SPL, IPL, and precuneus, produced positive math achievement effects. No regions in the left hemisphere parietal cortex were observed. A complete description of regional activation findings is provided in Table IV. All contrasts were corrected using a cluster-threshold procedure based on a Monte Carlo simulation to yield an overall $p \leq 0.05$ (Forman et al., 1995).

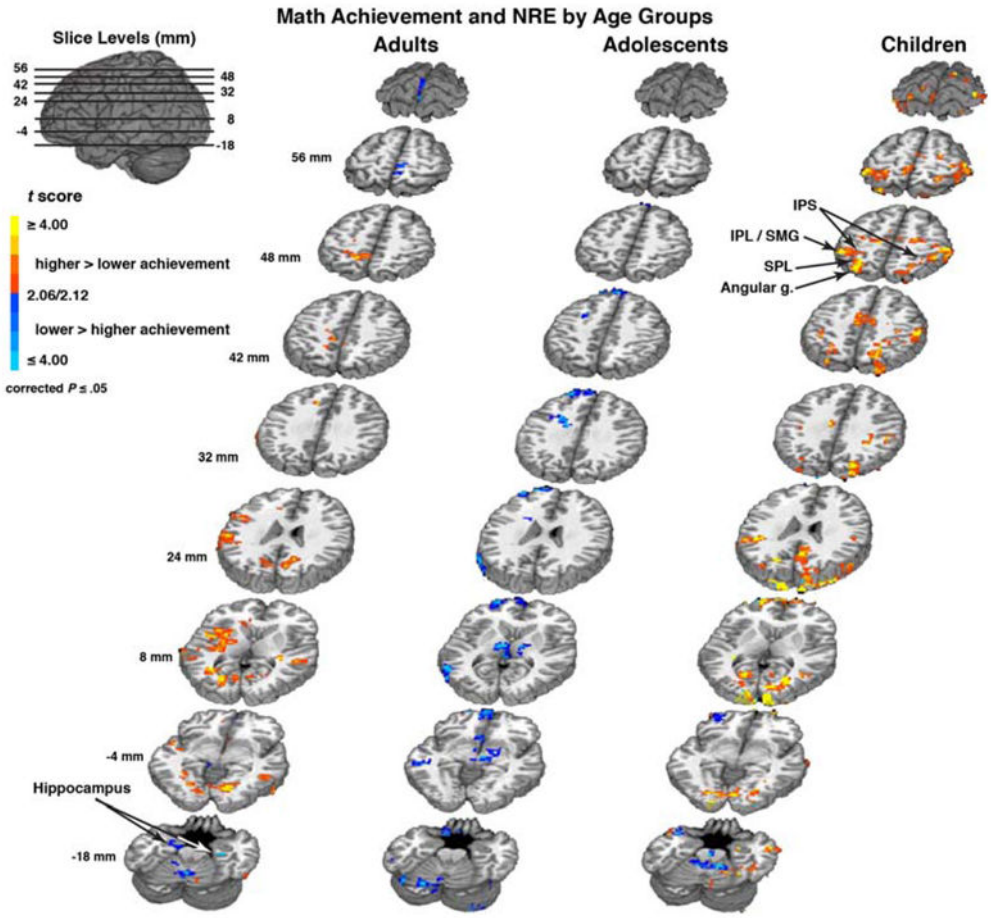

Figure 4.

Brain regions producing significant math achievement effects from the regression analyses against the NRE conducted separately for adults, adolescents, and children. (Left panel) Adults (≥18 years) showed no significant regional activation in lateral parietal cortex related to math achievement scores, but a significant negative correlation in bilateral hippocampus. (Middle panel) Adolescents (13–17 years) showed a negative relationship between achievement and the NRE in the left SPL, but no significant positive or negative correlations in the right or left IPS. (Right panel) Children (6–12 years) produced robust bilateral positive activation between math achievement and the NRE in parietal cortex, including IPS, IPL, and the SPL. The developmental differences in the findings suggest that children may engage separate brain systems during nonsymbolic numerosity that support some aspects of formal math achievement. A complete description of regional activation findings for each of the three groups together with the results of the pairwise contrast analyses are provided in Table V. All contrasts were corrected using a cluster-threshold procedure based on a Monte Carlo simulation to yield an overall $p \leq 0.05$ (Forman et al., 1995).

Table I

Demographic information of study participants and behavioral test scores including age correlations.

				Mean Woodcock-Johnson III Achievement Scaled Scores*					
Group	**N (F/M)**	**Mean Age (yrs)**	**Full Scale IQ**	**Broad Math**	**Calculation**	**Math Fluency**	**Quant. Concepts**	**Applied Problems**	**Letter-Word ID**
Adults (SD)	**16** (8/8)	**22.4** (3.8)	**121.1** (9.6)	**116.9** (13.4)	**120.3** (14.1)	**105.6** (12.4)	**113.4** (9.8)	**111.9** (13.1)	**106.1** (8.2)
Age Corr. (***r***) (p_B)			**−.227** (1.000)	**−.394** (.917)	**−.388** (.966)	**−.343** (1.000)	**−.223** (1.000)	**−.296** (1.000)	**−.074** (1.000)
Adolescents (SD)	**14** (5/9)	**15.4** (1.9)	**112.4** (12.8)	**111.2** (17.4)	**114.9** (20.4)	**99.2** (14.1)	**110.4** (13.2)	**110.4** (13.8)	**106.9** (12.0)
Age Corr. (***r***) (p_B)			**.214** (1.000)	**.162** (1.000)	**.220** (1.000)	**−.112** (1.000)	**.059** (1.000)	**.138** (1.000)	**−.010** (1.000)
Children (SD)	**14** (7/7)	**9.8** (1.8)	**112.6** (11.3)	**112.9** (18.7)	**111.4** (20.3)	**104.0** (12.7)	**108.9** (15.8)	**111.1** (13.4)	**110.7** (13.5)
Age Corr. (***r***) (p_B)			**.314** (1.000)	**.303** (1.000)	**.295** (1.000)	**.216** (1.000)	**.268** (1.000)	**.263** (1.000)	**.330** (1.000)
Full Sample (SD)	**44** (20/24)	**16.2** (5.8)	**115.7** (11.7)	**113.8** (16.3)	**115.7** (18.3)	**103.0** (13.0)	**111.0** (12.9)	**111.2** (13.1)	**107.8** (11.2)
Age Corr. (***r***) (p_B)			**.322** (.245)	**.115** (.1000)	**.212** (1.000)	**.022** (1.000)	**.166** (1.000)	**.031** (1.000)	**−.104** (1.000)

Note: Age ranges for the three groups are: adults = 18 – 34 years, adolescents = 13 – 17 years, and children 6 – 12 years. Full Scale IQ calculated from the two subtest version of Wechsler Abbreviated Scale of Intelligence (Matrix Reasoning and Vocabulary). Woodcock-Johnson III Scaled Scores: mean =100, SD = 15. Calc = Calculation. Quant. Concepts = Quantitative Concepts. Achievement data were unavailable for one child participant. The age-corrected Broad Math and Letter-Word ID test scores were used in analyses as measures of math and reading academic achievement. SD = standard deviation. Age Corr. (***r***) = Pearson correlation with age (natural logarithm transform). p_B = Bonferroni corrected *p* value of Pearson correlation coefficient (two-sided; 7 contrasts).

Hum Brain Mapp. Author manuscript; available in PMC 2015 June 23.

Table II

Correlation results between behavioral ratio effect (BRE), math achievement scores, and covariate tasks.

	Pearson Correlation						
	Woodcock-Johnson III Math Achievement Scales					**Covariates**	
Group	**Broad Math**	**Calculation**	**Math Fluency**	**Quant. Concepts**	**Applied Problems**	**Full Scale IQ**	**Letter-Word ID**
Adults							
RT - BRE	**.020**	**.291**	**−.172**	**−.277**	**−.129**	**−.463**	**−.249**
(*p*)	.940	.275	.525	.300	.634	.071	.353
Accuracy - BRE	**−.020**	**.216**	**−.385**	**−.218**	**−.057**	**−.266**	**−.183**
(*p*)	.940	.422	.140	.418	.833	.320	.498
Adolescents							
RT - BRE	**.098**	**−.002**	**.122**	**.022**	**.173**	**.045**	**.252**
(*p*)	.738	.995	.677	.941	.554	.878	.386
Accuracy - BRE	**−.332**	**−.302**	**−.290**	**−.367**	**−.269**	**−.074**	**−.042**
(*p*)	.246	.294	.315	.197	.353	.803	.885
Children							
RT - BRE	**.214**	**.229**	**.164**	**.076**	**.174**	**.146**	**−.229**
(*p*)	.462	.431	.575	.796	.551	.634	.432
Accuracy - BRE	**−.348**	**−.273**	**−.117**	**−.176**	**−.482**	**.182**	**−.048**
(*p*)	.222	.345	.689	.546	.081	.551	.871
Entire Sample							
RT - BRE	**.152**	**.228**	**.056**	**.022**	**.072**	**.057**	**−.134**
(*p*)	.326	.137	.717	.886	.642	.719	.386
Accuracy - BRE	**−.309***	**−.242**	**−.250**	**−.271**	**−.303***	**−.075**	**−.033**
(*p*)	.042	.113	.102	.076	.045	.631	.830

Note: Scaled scores (Mean = 100, SD = 15) were used for all test measures. *RT-BRE* = reaction time BRE. *p* = uncorrected *p* values of the Pearson correlation coefficient (two-tailed). The Broad Math Index score is a summary score calculated from the other four math achievement scores.

Table III

Brain regions observed in the regression of age on the neural ratio effect (NRE).

Region	BA	t_{max}	*Talairach Coordinates*			*MNI (SPM) Coordinates*		
			x	*y*	*z*	*x*	*y*	*z*
Positive effects (older > younger)								
Parietal								
R Intraparietal sulcus (IPS)		4.03	−34	−58	44	−35	−68	39
R Angular gyrus	39	2.83	−44	−58	44	−46	−68	39
R Inferior parietal lobule/Supramarginal gyrus	40	3.64	−46	−38	38	−48	−46	34
R Superior parietal lobule	7	4.07	−20	−70	38	−20	−80	30
R Precuneus	7/31	3.88	−14	−64	30	−14	−73	22
R Posterior cingulate		3.87	−4	−40	18	−3	−46	11
L Intraparietal sulcus (IPS)		3.69	28	−58	32	32	−67	24
L Angular gyrus	7	2.70	44	−58	36	49	−67	28
L Inferior parietal lobule/Supramarginal gyrus	40	2.62	40	−44	30	44	−52	23
L Precuneus	7	2.30	8	−74	32	10	−84	23
L Posterior cingulate		3.06	4	−38	18	5	−44	11
Frontal								
R Middle Frontal gyrus	46/10	4.09	−38	40	8	−40	40	9
R Inferior frontal gyrus	45	2.84	−38	32	18	−40	31	19
L Precentral gyrus	6	3.53	38	2	36	43	−3	35
Occipital-Temporal								
None observed		-	-	-	-	-	-	-
Subcortical/Cerebellum								
L Cerebellum Lobule V		4.55	2	−56	−22	3	−59	−35
Negative effects (younger > older)								
Parietal								
None observed		-	-	-	-	-	-	-
Frontal								
L Inferior frontal gyrus	47	2.59	44	16	0	49	15	−4

Region	BA	t_{max}	*Talairach Coordinates*			*MNI (SPM) Coordinates*		
			x	*y*	*z*	*x*	*y*	*z*
L Inferior frontal gyrus	44	2.28	56	8	24	62	4	22
Occipital-Temporal								
L Amygdala		2.29	28	−2	−12	31	−2	−19
L Superior Temporal gyrus	22	2.65	44	−2	−6	48	−3	−12
L Lingual gyrus	19	3.13	14	−56	−4	16	−61	−15
Subcortical/Cerebellum								
None observed		-	-	-	-	-	-	-

Note: The analysis used math achievement (Broad Math Index), Full Scale IQ, and reading achievement (Letter-Word Identification) as covariates. Positive effects indicate regions where higher achievement scores were associated with higher NRE values (i.e., greater numerosity acuity). BA = Brodmann's area. t_{max} = maximum *t* score in region. Positive coordinate values indicate left (x), anterior (y), and superior (z). Talairach coordinates follow the convention of the Talairach and Tournoux atlas (Talairach and Tournoux, 1988). MNI (SPM) equivalent coordinates were calculated using the GingerALE Convert Foci program (v. 2.3.1, http://www.brainmap.org/ale; Laird, et al., 2010; Lancaster, et al., 2007).

Table IV

Brain regions observed in the regression of math achievement on the neural ratio effect (NRE).

Region	BA	t_{max}	*Talairach Coordinates*			*MNI (SPM) Coordinates*		
			x	*y*	*z*	*x*	*y*	*z*
Positive effects (higher achievement > lower)								
Parietal								
R Intraparietal sulcus (IPS)		2.79	−26	−58	42	−39	−43	48
R Superior parietal lobule	7	3.32	−26	−68	48	−30	−66	51
R Inferior parietal lobule/Supramarginal gyrus	40	3.64	−46	−40	44	−49	−36	47
R Precuneus	7	3.95	−10	−70	38	−13	−69	45
Frontal								
R Superior frontal gyrus	8	2.94	−22	22	38	−25	29	35
R Middle frontal gyrus	6	3.46	−28	2	50	−32	9	50
R Medial Superior frontal gyrus	10	3.79	−10	64	12	−12	71	2
Occipital-Temporal								
R Inferior temporal gyrus (posterior)	37	3.81	−55	−40	−24	−60	−43	−28
R Lingual gyrus	18	3.35	−10	−70	0	−12	−73	2
R Cuneus	17/18	4.40	−14	−68	12	−17	−70	15
R Middle occipital gyrus	19	3.24	−38	−74	20	−43	−75	25
R Middle temporal gyrus (temporal pole)	38	3.23	−40	14	−30	−44	13	−40
R Inferior temporal gyrus (temporal pole)	21	2.54	−38	2	−28	−42	1	−37
L Lingual gyrus	18/19	2.92	22	−62	0	22	−65	2
L Cuneus	17/18	4.11	14	−70	8	14	−72	12
Subcortical/Cerebellum								
R Cerebellum Lobule VIIa Crus I/II		3.48	−40	−56	−36	−44	−62	−40
R Cerebellum Lobule VI		2.85	−10	−70	−18	−12	−75	−18
Negative effects (lower achievement > higher)								
Parietal								
None observed		-	-	-	-	-	-	-
Frontal								

Hum Brain Mapp. Author manuscript; available in PMC 2015 June 23.

Region	BA	t_{max}	*Talairach Coordinates*			*MNI (SPM) Coordinates*		
			x	*y*	*z*	*x*	*y*	*z*
R Middle frontal gyrus	10	3.07	−22	52	26	−25	64	18
R Superior frontal gyrus	9	2.76	−14	58	26	−16	66	18
Occipital-Temporal								
None observed		-	-	-	-	-	-	-
Subcortical/Cerebellum								
Bilateral Cerebellum Lobules I-IV		4.17	−8	−40	−16	−10	−43	−18

Note: The analysis used age, Full Scale IQ, and Woodcock-Johnson III Letter-Word Identification scaled scores as covariates. Positive effects indicate regions where higher achievement scores were associated with higher NRE values (i.e., greater numerosity acuity). BA = Brodmann's area. t_{max} = maximum *t* score in region. Positive coordinate values indicate left (x), anterior (y), and superior (z). See Table III for description of coordinates.

Table V

Results from regression of math achievement on the neural ratio effect (NRE) for adults, adolescents, and children separately.

Region	BA	t_{max}	*Talairach Coordinates*			*MNI (SPM) Coordinates*		
			x	*y*	*z*	*x*	*y*	*z*
Adults (≥18 years)								
Positive effects (higher achievement > lower)								
Parietal								
L Precuneus # †	7	5.94	14	−52	44	13	−49	50
L Inferior parietal lobule/Supramarginal gyrus †	40	2.84	56	−34	20	59	−33	22
Frontal								
L Inferior frontal gyrus	44	4.00	50	4	20	53	8	18
L Anterior cingulate # †	24/32	3.18	10	32	2	10	36	−6
L Insula (middle)		2.44	32	4	8	33	6	4
Occipital-Temporal								
R Lingual gyrus # †	18	4.88	−16	−68	−6	−19	−71	−5
R Inferior temporal gyrus	37	4.13	−56	−50	−10	−62	−53	−12
R Middle Temporal gyrus # †	22	4.65	−46	−34	2	−51	−34	0
R Superior temporal gyrus #	22	3.49	−50	−34	8	−55	−34	7
R Precuneus (inferior)	18	3.47	−10	−70	24	−12	−70	29
R Cuneus	18	2.59	−10	−68	8	−12	−70	11
L Lingual gyrus †	18	3.11	20	−70	−4	20	−73	−1
L Superior temporal gyrus # †	22	3.31	50	−28	2	−55	−28	−1
L Middle temporal gyrus	22	3.86	58	−32	2	−64	−32	0
L Insula (posterior) # †		2.83	38	−22	8	40	−21	7
L Cuneus	18	3.76	16	−74	8	16	−76	12
Subcortical/Cerebellum								
L Caudate (anterior) #		2.70	14	14	14	14	18	10
L Putamen		3.26	20	−10	8	20	−8	6
Negative effects (lower achievement > higher)								

Region	BA	t_{max}	Talairach Coordinates			MNI (SPM) Coordinates		
			x	*y*	*z*	*x*	*y*	*z*
Parietal								
R Paracentral lobule (#)	4	3.34	−4	−38	56	−6	−33	61
R Precuneus (#) (†)	7	3.40	−4	−50	56	−6	−46	63
Frontal								
R Anterior cingulate (#)	32	3.90	−4	32	−10	−5	34	−19
Occipital-Temporal								
R Hippocampus (#) (†)		5.99	−26	−16	−12	−29	−17	−17
L Hippocampus (#)		2.44	22	−10	−16	23	−11	−21
Subcortical/Cerebellum								
L Cerebellum hemisphere Lobule V (#)		2.28	4	−58	−16	3	−62	−16
Adolescents (13–17 years)								
Positive effects (higher achievement > lower)								
None observed								
Negative effects (lower achievement > higher)								
Parietal								
None observed								
Frontal								
R Anterior cingulate (#) (*)	32	3.57	−4	20	−6	−5	22	−14
R Paracentral gyrus (#) (*)	4	3.12	−8	−22	60	−11	−16	64
L Middle frontal gyrus (#) (*)	44	3.78	28	10	30	29	15	28
L Middle frontal gyrus (rostral) (*)	9	3.92	22	52	30	23	60	24
L Middle frontal gyrus (#)	6	3.24	26	4	42	26	10	42
L Superior frontal gyrus (rostral) (#) (*)	9	4.30	14	58	26	14	66	18
L Anterior cingulate (#) (*)	24/32	5.80	4	16	−6	3	18	−13
L Paracentral gyrus (#) (*)	4	3.73	8	−26	60	7	−20	65
Occipital-Temporal								
L Middle temporal gyrus (#) (*)	20/21	4.38	58	−20	−12	62	−21	−15

Region	BA	t_{max}	Talairach Coordinates			MNI (SPM) Coordinates		
			x	*y*	*z*	*x*	*y*	*z*
L Middle temporal gyrus (#) (*)	37	4.28	50	−62	8	53	−64	12
Subcortical/Cerebellum								
R Thalamus (prefrontal) (#) (*)		4.18	−8	−16	2	−10	−15	−1
R Cerebellum Lobule VIIa Crus I (#) (*)		5.91	−22	−70	−24	−25	−75	−24
L Cerebellum Lobule VIIa Crus I (#) (*)		3.88	20	−76	−18	21	−81	−16
Children (6 – 12 years)								
Positive effects (higher achievement > lower)								
Parietal								
R Intraparietal sulcus (IPS) * †		3.76	−26	−58	44	−30	−56	50
R Superior parietal lobule *	7	4.12	−22	−68	44	−26	−66	51
R Inferior parietal lobule/Supramarginal gyrus †	40	3.50	−50	−32	32	−56	−28	33
R Precuneus * †	7	4.14	−4	−62	26	−6	−62	31
R Postcentral gyrus	2	4.84	−52	−25	42	−58	−21	44
L Intraparietal sulcus (IPS) *		4.37	26	−58	42	26	−56	48
L Superior parietal lobule * †	7	5.61	32	−58	50	33	−55	57
L Angular gyrus *	39	3.94	40	−62	48	45	−59	54
L Inferior parietal lobule/Supramarginal gyrus * †	40	6.68	46	−44	48	48	−41	54
L Precuneus * †	7	3.60	8	−46	56	7	−42	62
Frontal								
R Superior frontal gyrus	6	3.51	−22	20	50	−25	28	48
R Middle frontal gyrus *	6	4.21	−22	−14	56	−26	−8	58
R Precentral gyrus †	3	3.50	−38	−32	56	−43	−27	60
R Middle cingulate cortex †	6	3.45	−8	−14	44	−10	−9	45
R Middle frontal gyrus * †	10	3.14	−26	56	−12	−29	60	−24
L Middle frontal gyrus * †	10	6.19	28	56	12	29	62	3
L Precentral gyrus * †	4	3.14	22	−20	50	22	−15	53

Region	BA	t_{max}	Talairach Coordinates			MNI (SPM) Coordinates		
			x	*y*	*z*	*x*	*y*	*z*
L Middle cingulate gyrus †	6	3.77	8	−10	38	7	−5	39
Occipital-Temporal								
R Lingual gyrus/Calcarine * †	17/18	4.67	−10	−82	−4	−12	−86	−1
R Middle occipital gyrus *	18	3.54	−28	−80	−6	−32	−84	−4
R Middle occipital gyrus * †	18	4.00	−32	−86	12	−36	−89	17
R Posterior cingulate * †	30	3.25	−14	−64	12	−17	−65	15
R Cuneus *	18	5.40	−14	−86	20	−17	−88	26
R Fusiform gyrus *	37	2.88	−40	−40	−18	−44	−43	−21
R Middle temporal gyrus (posterior) * †	37	3.54	−50	−62	12	−55	−63	14
L Lingual gyrus †	18	5.00	8	−82	−6	7	−86	−3
L Cuneus	17/18	4.45	14	−68	8	14	−70	12
L Superior temporal gyrus †	22	3.97	52	−40	18	55	−39	20
L Superior temporal gyrus	41	4.02	38	−38	14	40	−38	16
Subcortical/Cerebellum								
R Cerebellum Lobule VIIa Crus I * †		4.16	−34	−58	−28	−38	−63	−30
Negative effects (lower achievement > higher)								
Parietal								
None observed		-	-	-	-			
Frontal								
L Middle frontal gyrus (*) (†)	10	3.72	34	50	0	36	55	−9
Occipital-Temporal								
Superior temporal gyrus (temporal pole) (*)	38	3.76	44	−8	−16	47	−9	−21
Subcortical/Cerebellum								
R Cerebellum Lobule I–IV (*)		3.90	−10	−40	−18	−12	−39	19
L Cerebellum Lobule I–IV		4.20	10	−40	−16	10	−43	−18

Note: Regressions used age, together with Full Scale IQ and Woodcock-Johnson III Letter-Word Identification scaled scores as covariates to control for overall cognitive ability and non-math achievement. Pairwise contrasts used ANCOVA with FSIQ and WJIII- Letter-Word ID as covariates; $p < .05$: Positive effects:

[*] regression slope > Adults;

[†] regression slope > Adolescents;

[#] regression slope > Children; Negative effects:

[(*)] regression slope < Adults;

[(†)] regression slope < Adolescents;

[(#)] regression slope > Children.

BA = Brodmann's area. t_{max} = maximum *t* score in region. Positive coordinate values indicate left (x), anterior (y), and superior (z). See Table III for additional description of coordinates.